Insights into fucose metabolism: SLC35C1-independent fucosylation discriminates against mannose-derived GDP-fucose

Edyta Skurska
University of Wroclaw: Uniwersytet Wroclawski
Bożena Szulc
University of Wroclaw: Uniwersytet Wroclawski
Dorota Maszczak-Seneczko
University of Wroclaw: Uniwersytet Wroclawski
Maciej Wiktor
University of Wroclaw: Uniwersytet Wroclawski
Wojciech Wiertelak
University of Wroclaw: Uniwersytet Wroclawski
Mariusz Olczak (mariusz.olczak@uwr.edu.pl)
University of Wroclaw: Uniwersytet Wroclawski https://orcid.org/0000-0001-8629-6364

Research Article

Keywords: SLC35C1, SLC35C2, GDP-fucose synthesis, fucose supplementation, LADII, nucleotide sugar transporter

Posted Date: November 23rd, 2021

DOI: https://doi.org/10.21203/rs.3.rs-1096518/v1

Abstract

Mutations in the *SLC35C1* gene, encoding the Golgi GDP-fucose transporter, cause leukocyte adhesion deficiency II (LADII). Fucosylation improvement in LADII patients treated with fucose suggests the existence of an SLC35C1-independent route of GDP-fucose transport, which still remains a mystery. Here, we developed and characterized a human cell-based model deficient in the SLC35C1 activity. The knockout cells displayed low but detectable levels of fucosylation. Strikingly, the fucosylation defect was almost completely reversed upon treatment with millimolar concentrations of fucose. Even if fucose was supplemented at nanomolar concentrations, it was still incorporated into glycans by the knockout cells. We also found that the SLC35C1-independent transport preferred the salvage pathway over the *de novo* pathway as a source of GDP-fucose. Our results imply that the Golgi systems of GDP-fucose transport discriminate between the substrate pools obtained from different metabolic pathways, which suggests a functional connection between nucleotide sugar transporters and nucleotide sugar synthetases.

Introduction

Fucose is an abundant component of many N- and O-glycans as well as some glycolipids. Except for O-fucosylation, where it is the first sugar in a sequence, fucose is always a terminal sugar in the structure of oligosaccharides. Fucose can be attached to other sugars or proteins *via* one of four types of glycosidic bonds: α-1,2, α-1,3, α-1,4 and α-1,6. In N-glycans, fucose is predominantly α-1,6-linked to the first (Asn-bound) *N*-acetylglucosamine residue. Such type of fucose is referred to as a core fucose and it is incorporated into the oligosaccharide structure only after the attachment of at least one *N*-acetylglucosamine residue to mannose. For a broader overview of the consecutive steps of N-glycan processing the reader is kindly referred to [1].

Fucosylated oligosaccharides have many biologically relevant functions. AB0 blood group antigens are among the best known fucosylated glycans. O-linked fucose may affect certain ligand-receptor interactions involved in signal transduction. Fucose decorates certain oligosaccharides that are exposed on the surface of leukocytes and serve as ligands for selectins. Binding of the latter to the former initiates the leukocyte adhesion cascade, a multi-step process of leukocyte migration to the site of injury or infection.

Incorporation of fucose into glycoconjugates is mediated by fucosyltransferases, which are predominantly Golgi-resident type II membrane proteins. Fucosyltransferases use the active form of fucose, i.e. GDP-fucose, as a substrate. GDP-fucose is synthesized in the cytoplasm by the two different pathways (shown in Fig. 1). The main source of this nucleotide sugar is the so-called *de novo* pathway which is estimated to provide 90-95% of the total GDP-fucose pool in the cell [2, 3]. The primary substrate for this three-step pathway is mannose. First, this monosugar is converted into GDP-mannose, then GDP-D-mannose 4,6-dehydratase (GMDS) converts GDP-mannose to GDP-4-keto-6-deoxymannose. This keto intermediate is then converted into GDP-fucose by an epimerase/reductase enzyme complex termed the FX protein or GDP-L-fucose synthase (also known as GFUS, FCL, SDR4E1 or TSTA3) [4].

The second, alternative way of GDP-fucose synthesis is the so-called salvage pathway. This route uses cytoplasmic pool of free fucose, which on the one hand is recovered from glycoconjugates by lysosomal α-fucosidase activity, and on the other hand is supplied from the environment. Little is known about the fucose transport system from the extracellular space to the interior of the cell, but it appears to function through facilitated diffusion through specific channel(s) [5]. The first step of the salvage pathway involves an ATP-dependent synthesis of fucose-1-phosphate by the fucokinase (FUK; also known as FCSK) enzyme. GDP-fucose pyrophosphorylase (FPGT), the second enzyme acting in the pathway, catalyzes the conversion of fucose-1-phosphate and GTP to GDP-fucose [6]. As already mentioned, it is estimated that only 5-10% of the total GDP-fucose pool is synthesized by this pathway [2, 3].

To reach lumenally oriented catalytic centers of fucosyltransferases, GDP-fucose has to be transported across the Golgi membrane. This function is thought to be played by GDP-fucose-specific nucleotide sugar transporters (NSTs), which are hydrophobic type III membrane proteins with 6-10 transmembrane domains. NSTs are believed to act as antiporters; an imported nucleotide sugar is exchanged with the corresponding nucleoside monophosphate [7]. After reaching the Golgi lumen, the activated monosugar constitutes a substrate for a respective glycosyltransferase, which attaches the monosugar to an acceptor, whereas the released nucleoside diphosphate is broken down into a nucleoside monophosphate and an inorganic phosphate [8].

In mammals, the role of the main GDP-fucose transporter is attributed to the product of the *SLC35C1* gene, which was identified by two independent groups in 2001 [9, 10]. Although SLC35C1 is thought to be the major transporter in mammals, GDP-fucose has also

been shown to translocate through its homolog, SLC35C2. SLC35C2 was shown to localize predominantly in the Golgi, but a small subset of it was found in the endoplasmic reticulum (ER) and ERGIC (ER-Golgi intermediate compartment). SLC35C2 is specifically required for O-fucosylation of certain proteins including the Notch receptor, which in turn does not require the SLC35C1 activity [11, 12].

Leukocyte adhesion deficiency II (LADII) is a rare autosomal recessive genetic disease characterized by an overall reduction in fucosylation of glycoconjugates. This syndrome is caused by mutations in the *SLC35C1* gene [13]. The characteristic symptoms of this disease include psychomotor retardation, facial dysmorphism, Bombay phenotype, short stature, immunodeficiency, leukocytosis as well as recurrent and frequent bacterial infections [14]. LADII was first diagnosed in 1992 [15]. To date, 19 individuals bearing inactivating mutations in the *SLC35C1* gene have been reported [14–23] with a predominance of point mutations.

The concept of using exogenous fucose to improve fucosylation in LADII patients was first raised in 1998. Pioneering experiments were performed with lymphoblastic cells obtained from one of the patients bearing the Arg147Cys mutation in the SLC35C1 amino acid sequence. Supplementation of the cell culture with 10 mM fucose for 5 days triggered an increase in the number of fucosylated structures [24]. These results paved the way to the concept of using fucose supplementation in patients themselves. Since 1999, several LADII patients were treated with oral fucose. For some of them such treatment was successful, resulting in an improvement in psychomotor development and a reduction in neutrophil count [22, 25]. However, in the case of two LADII patients fucose supplementation failed to improve their condition [20, 26]. The administered doses of fucose varied from 25 to 2000 mg/kg body weight [20, 25, 26]. An improvement in fucosylation was also achieved when the LADII patient-derived fibroblasts were cultured in the presence of 0.1-10 mM fucose [18].

To explain the effectiveness of the fucose treatment in responsive LADII patients, it was postulated that the mutant SLC35C1 variants display some residual transport activity [9]. Therefore, a therapy causing an increase in the cytosolic concentration of this nucleotide sugar could potentially allow to overcome the insufficient transporting activity of the defective SLC35C1 variants. However, a direct proof for an increase in the cytosolic GDP-fucose concentration in the fucose-fed cells bearing mutations in the *SLC35C1* gene has not been presented to date. An alternative hypothesis to explain the efficiency of the oral fucose therapy could be the existence of an accessory GDP-fucose transport system, however, no such route has been identified so far.

In 2007, a knockout-based study conducted in mice revealed that the fucose treatment works even in the absence of SLC35C1 [27]. These findings for the first time suggested the existence of an SLC35C1-independent GDP-fucose transport into the Golgi, as the observed effect could no longer be explained by a residual activity of the SLC35C1 mutants. It was hypothesized that the SLC35C1 deficiency could be overcome by the SLC35C2 activity, but this has never been proved. In general, no studies that could possibly explain this phenomenon in bigger detail have been undertaken so far.

Since the responsiveness of the cells completely devoid of the SLC35C1 activity to fucose treatment has not been elucidated to date, here we have undertaken a more-in-depth investigation of this intriguing effect. Within our general interest in the metabolism of fucose and protein fucosylation, specific goals included: (i) generation of single SLC35C1 and double SLC35C1/SLC35C2 knockouts, (ii) optimization of fucose feeding conditions, (iii) establishment of a method allowing quantification of the extent of N-glycan fucosylation, (iv) structural characterization of N- and O-glycans produced by the wild-type and knockout cells, (v) investigation of N-glycan fucosylation in response to various ranges of exogenous fucose concentrations, (vi) single-point and time-course analyses of intracellular GDP-fucose concentration in control and fucose-fed cells, (vii) determination of the contribution of *de novo* and salvage GDP-fucose biosynthetic pathways to fucose incorporation into N-glycans in the wild-type and knockout cells and (viii) assessment of a potential cellular genetic response to fucose supplementation.

In this study we have developed an approach coupling exoglycosidase digestion with HPLC to quantify the percentage of the core-fucosylated N-glycans with a great precision. We showed that in the knockout cells the core fucosylation of N-glycans is greatly reduced but can be nearly completely restored by supplementing the cells with millimolar concentrations of fucose. Supplementation with 5 mM fucose caused a significant increase in the intracellular GDP-fucose concentration, regardless of the presence/absence of GDP-fucose transporters. Next, by feeding low (nanomolar) concentrations of radioactive fucose and mannose into the culture medium we were able to follow the metabolic fate of the supplemented compounds and attribute radioactivity to fucosylated structures using our HPLC-based method. Surprisingly, the SLC35C1 knockouts showed a dramatic impairment of the ability to incorporate mannose-derived radioactivity into the fucosylated N-glycans. In sharp contrast, they were able to incorporate even higher

quantities of radiolabeled fucose than the wild-type cells. To explain these observations we hypothesize that in the SLC35C1 knockouts the salvage pathway is preferred over the *de novo* pathway as a source of GDP-fucose for fucosylation of N-glycans. We have also investigated potential genetic response of the SLC35C1 knockouts to fucose treatment. No major gene up/down-regulations were observed. Finally, we excluded SLC35C2 as an alternative supplier of GDP-fucose for N-glycan fucosylation.

Results

Generation of the single SLC35C1 and double SLC35C1/SLC35C2 knockouts

To develop a research model for our study, an SLC35C1 knockout (C1KO) was generated in two human cell lines, i.e. HEK293T and HepG2 using the CRISPR/Cas9 approach. Additionally, a double SLC35C1/SLC35C2 knockout (C1/C2KO) was developed in HEK293T cells to evaluate the influence of SLC35C2 protein on the N- and O-glycosylation in the SLC35C1 knockout cells and to examine the effect of fucose treatment in cells lacking both GDP-fucose transporters. The knockouts were confirmed by RT-PCR performed on total RNA and PCR performed on genomic DNA (Fig. S1A and S1B). The SLC35C1 knockout was additionally verified on the protein level using an anti-SLC35C1 antibody by western blotting (Fig. S1C) as well as by double staining with the latter antibody and fucose-specific *Aleuria aurantia* lectin (AAL, Fig. S1D).

To show that the knockout phenotype was specifically associated only with the disruption of the *SLC35C1* gene, we have also developed SLC35C1-deficient clones stably over-expressing a recombinant, HA-tagged SLC35C1 (in both HEK293T and HepG2 cell lines). The overexpression was confirmed by western blotting performed on cell lysates using an anti-HA antibody (Fig. S1E). The obtained stable transfectants were also subjected to immunostaining to confirm the Golgi localization of the over-expressed protein (Fig. S1F).

Optimization of fucose supplementation conditions

In order to establish a system to study the effect of fucose supplementation on the restoration of fucosylation in the SLC35C1 knockouts, feeding parameters, i.e. fucose concentration in the culture medium as well as duration of the treatment, had to be optimized. In the first stage we employed a dot blot analysis using AAL lectin (Fig. 2A, 2B). Several concentrations of fucose were tested, i.e. 0.5, 1, 5 and 10 mM (concentration range inspired by [18]). We found that after 5 days, 5 mM concentration was sufficient to substantially restore fucosylation of glycoconjugates in the SLC35C1 knockouts. AAL stainings performed on the SLC35C1 knockouts cultured in the presence of 5 mM fucose for 0-48 h demonstrated that the level of fucosylation gradually increased over time and an optimum (i.e. fucosylation compared to the wild-type) was reached after 24 h. After another 12 h, however, the cells became overloaded with aggregated fucose-containing structures (Fig. 2C).

Since the lectin-based analysis does not allow for quantification of the observed fucosylation defects/rescue effects, we have established a new, robust method, based on exoglycosidase digestions followed by HPLC separation, that allows quantification of the degree of the α-1,6-fucosylation (core fucose). In our approach, we used specific glycosidases to reduce all multi-branched complex-type N-glycan species into a simple biantennary $(GlcNAc)_2(Man)_3$ structure, either fucosylated or non-fucosylated (Fig. 2D, 2E). Then by taking a ratio of the area of the fucosylated peak over the sum of areas of both peaks (fucosylated and non-fucosylated) we have determined the percentage of fucosylated structures for each sample. To confirm that the fucosylated peak contains only $(GlcNAc)_2(Man)_3Fuc$ structure, the α- fucosidase digestion was performed (Fig. 2F)

By employing our method we tested supplementation of selected fucose concentrations (50 μM - 100 mM) for different time periods (1-5 days) in the wild-type and SLC35C1 knockout HEK293T cells. Feeding the cells with 50 μM or 1 mM fucose even for as long as 5 days was not sufficient to restore the wild-type α-1,6-fucosylation level in the SLC35C1 knockout cells. Only supplementation of the SLC35C1 knockout cells with 5 mM fucose restored fucosylation phenotype to a level comparable to the wild-type, but at the same time it did not affect core fucosylation in the wild-type cells. At the same time, supplementation with a very high fucose concentration (100 mM) did not increase the level of core fucosylation in the wild-type cells (Fig. 2G). Therefore, for the final experiments, the conditions of 5 mM fucose and 24 h were selected.

Supplementation of fucose in the knockout cells significantly increases α-1,6-fucosylation of N-glycans

We quantified α-1,6-fucosylation of N-glycans in all modified cell lines. From the analysis of the HEK293T cells we could conclude that: (i) the native level of core fucosylation in the non-fed wild-type cells oscillates around ~75% and is compromised to ~8-10% in the single SLC35C1 and double SLC35C1/SLC35C2 knockouts, (ii) ectopic expression of the HA-tagged SLC35C1 in the single SLC35C1 knockouts restores the wild-type phenotype, (iii) nearly complete α-1,6 fucosylation (~60%) can be achieved in both single SLC35C1 and double SLC35C1/SLC35C2 knockouts upon administration of 5 mM fucose for 24 h (Fig. 3A). As anticipated, similar observations were made for the HepG2 cells (Fig. 3B). MALDI-TOF analysis of N-glycan structures confirmed those results, showing the presence of a fucosylated structure in the SLC35C1 knockouts and restoration of fucosylated structures after fucose feeding (Fig. S2).

During the separation and purification of N-glycans, there is a possibility of contamination with the oligosaccharides derived from serum glycoproteins contained in the culture medium. To address this problem, the N-glycans derived from an engineered, ectopically expressed and secreted reporter glycoprotein, Secreted Alkaline Phosphatase (SEAP), were also analyzed. The method for SEAP isolation efficiently prevents contamination with serum glycoproteins [28]. From the analysis of α-1,6-fucosylated N-glycans derived from the SEAP overexpressed in the wild-type and knockout HEK293T cells we concluded that in the knockouts α-1,6-fucosylation of SEAP-derived N-glycans is still present (~3-5%) and supplementation of 5 mM fucose for 24 h restore α-1,6-fucosylation in these cells. Interestingly, the level of α-1,6-fucosylation observed in the wild-type and knockout cells was higher than it was in the wild-type before supplementation, which could be a specific response of the overexpressed SEAP on the supplementation (Fig. 3C). As anticipated, similar observations were made for the HepG2 cells (Fig. 3D).

Supplementation of fucose restores fucosylation of O-glycans in the knockout cells

Certain mucin-type O-glycans are also fucosylated. The effect of GDP-fucose transport deficiency on this type of oligosaccharides was only investigated using lectins [27]. Therefore, we have additionally analyzed cellular mucin-type O-glycans using the CORA strategy [29].

From the analysis of the HEK293T cells we could conclude that: (i) in the wild-type cells 2 among 8 of the identified glycans were fucosylated (m/z values of ~1218 and ~1578; Fig. 4A), (ii) both fucosylated species were absent in the knockouts in which only their non-fucosylated counter-partners were detected (m/z values of ~1044 and 1404), (iii) a new fucosylated species was observed in the knockouts (m/z~ 1013, Fig. 4B, C), (iv) supplementation with 5 mM fucose for 24 h led to a re-appearance of the fucosylated species in the knockouts. Surprisingly, after fucose supplementation additional fucosylated species were observed in the wild-type and SLC35C1 knockout cells, but not in the double SLC35C1/SLC35C2 knockout (Fig. 4D, E, F). In the case of HepG2 cells the fucosylated O-glycan species were not produced by the SLC35C1 knockout. However, in contrast to HEK293T cells, fucose supplementation of the wild-type HepG2 cells did not have an influence on fucosylated O-glycans (Fig. 4G-J). The observed differences could be cell line-specific.

These results prove the role of SLC35C1 in the process of mucin-type O-glycan fucosylation and goes in line with the observations made for the N-glycans. Importantly, supplementation with 5 mM fucose for 24 h restored fucosylation of O-glycans in the single SLC35C1 and double SLC35C1/SLC35C2 knockout cells.

Supplementation of fucose increases intracellular GDP-fucose concentration

Although it is anticipated that in the SLC35C1-deficient cells the exogenous fucose efficiently enters the cells and becomes converted into GDP-fucose, to our best knowledge this phenomenon was neither quantified. For separation and quantitative analysis of nucleotide sugars we employed a modified ion-pair solid-phase extraction and HPLC strategy developed by Räbinä et al. [30]. Our results demonstrated that in the non-fed HEK293T cells the intracellular concentration of GDP-fucose oscillated around ~5 μM, regardless of the genotype (wild-type or single/double knockout). This shows that GDP-fucose transporter deficiency of the SLC35C1 knockout did not cause a GDP-fucose accumulation. This is in contrast to the research conducted on the SLC35A1 (CMP-sialic acid transporter) knockout, for which such an effect was observed [31]. Importantly, upon fucose supplementation, GDP-fucose concentration increased ~40-50-fold in all HEK293T cell lines, up to ~200-250 μM (Fig. 5A). Similar experiment was performed for HepG2 cells where the basal concentrations of GDP-fucose were slightly higher (~10 μM) and the effect of supplementation was somewhat less pronounced (~15-fold, up to ~150 μM) (Fig. 5B). Based on these findings we concluded that the externally supplemented fucose efficiently enters the cytoplasm and is being converted to GDP-fucose in all tested cell lines.

Supplementation of fucose causes dynamic changes in fucose metabolism

As a follow-up on these remarkable increases in the GDP-fucose concentration in response to fucose supplementation, a measurement of the intracellular concentration of fucose was undertaken. Using an enzymatic assay we have determined the intracellular concentration of fucose at a level of ~1 mM in the SLC35C1-knockouts supplemented with 5 mM fucose. From these numbers one can postulate an approximate equilibrium of 5 mM / ~1 mM / ~0.2 mM for the extracellular fucose / intracellular fucose / intracellular GDP-fucose.

Subsequently, in order to study the GDP-fucose turnover, the time-course evaluation of the intracellular GDP-fucose concentration was performed in the HEK293T wild-type and SLC35C1 knockout cells over the course of 24 h. As shown in Fig. 5C, GDP-fucose concentrations close to the maximum levels of ~250 µM were reached as soon as after 6-12 h since the beginning of the supplementation. However, when the supplementation was terminated, GDP-fucose concentration remained stable for ~8 h and then started to gradually decline towards basal levels (Fig. 5D). These observations were then correlated to the glycophenotype investigated using AAL fluorescent staining (Fig. 5E). After 24 h of supplementation fucosylation was strongly pronounced which was manifested by an efficient lectin binding (Fig. 5E, 0h). Withdrawal of the monosaccharide from the culture medium caused a gradual reduction of fucosylation which was no longer detectable after 48 h.

Having discovered that supplementation of 5 mM fucose for 24 h led to a drastic increase in the intracellular GDP-fucose concentration, we next examined how different fucose concentrations will affect the intracellular GDP-fucose concentration and core fucosylation of N-glycans. Therefore, we cultured the wild-type and SLC35C1 knockout HEK293T cells in the presence of 0 - 5 mM fucose for 24 h and determined the GDP-fucose concentrations for each of the tested fucose concentrations. A visible increase in the GDP-fucose concentration required the supplementation of at least 0.2 - 1 mM fucose (Fig. 5F). Then we have demonstrated that in the SLC35C1 knockouts core fucosylation of N-glycans increases proportionally to the concentration of the intracellular GDP-fucose (Fig. 5G). The finding that increasing GDP-fucose concentration in the wild-type cells does not have any effect on the core fucosylation of N-glycan goes in line with our previous results. Our data demonstrate that a significant increase in the intracellular GDP-fucose concentration is necessary to restore core fucosylation of N-glycans in the SLC35C1 knockouts.

Our data showed that GDP-fucose derived from the salvage pathway is efficiently utilized in the SLC35C1 and SLC35C1/C2 knockout cells. By supplementation of cells with small concentration of radiolabeled [6-^{3}H]fucose, we were able to track the biosynthesis of GDP-fucose *via* the salvage pathway and incorporation of fucose into N-glycans. We showed that the radioisotope incorporated into core fucosylated N-glycans produced by all tested cell lines (Fig. 6A, B, C). It means that even small amounts of exogenous fucose can be incorporated into core fucosylated N-glycans in the SLC35C1 and SLC35C1/C2 knockouts. Based on the known total radioactivity of the fucose substrate fed to the cells and on the measured radioactivity in the isolated fraction of the core fucosylated N-glycans, one can estimate the efficiency of the radioisotope incorporation (Fig. 6D, E). The fact that the higher percentage of core fucose was incorporated into N-glycans by the knockout cells may suggest a greater contribution of the GDP-fucose derived from the salvage pathway in the knockout cells as compared to the wild-types. We also observed that the biosynthesis of GDP-fucose in the salvage pathway occurs in both the wild-type and knockout cells (Fig. 6F, G, H). Altogether, these results may suggest the preferential usage of the salvage pathway-produced GDP-fucose for the N-glycan fucosylation in the SLC35C1 knockout cells.

Supplementation of millimolar mannose does not increase the intracellular GDP-fucose concentration

We discovered that only when we increase intracellular GDP-fucose, a restoration of the core fucosylation of N-glycans in the SLC35C1 knockout cells is observed. We next tested if 5 mM mannose (another source of GDP-fucose in the cells) feeding for 48 h will increase the intracellular GDP-fucose concentration. In both the wild-type and knockout cells mannose supplementation caused an increase in the intracellular GDP-mannose concentration (from ~100 µM to ~220 µM in the wild-type and from ~180 µM to ~330 µM in the knockout; Fig. 7A). In contrast, no mannose to GDP-fucose conversion was observed in the mannose-fed cells, regardless of their genotype (Fig. 7B). Having found that feeding the cells with 5 mM mannose does not cause any increase in the intracellular GDP-fucose concentration we next decided to examine whether radiolabeled mannose supplemented in low (nanomolar) concentrations will be converted into GDP-fucose, i.e. to verify, whether the *de novo* pathway works properly in the analyzed cells. Importantly, both the wild-type and SLC35C1 knockout cells efficiently converted the supplemented radiolabeled mannose into GDP-fucose (Fig. 7C, D).

The *de novo* and salvage pathways differentially contribute into N-glycan fucosylation in the SLC35C1 knockout cells

To compare the relative contribution of different GDP-fucose biosynthesis pathways into the N-glycan fucosylation, the wild-type and SLC35C1-deficient HEK293T cells were cultured in the presence of nanomolar concentrations of either radioactive fucose (salvage pathway) or radioactive mannose (*de novo* pathway). However, apart from conversion into GDP-fucose, mannose can be also processed into other nucleotide sugars, e.g. GDP-mannose, and as such incorporated into the complex type N-glycans. To address this problem, we have established a new approach in which the N-glycans are first digested with α-fucosidase, then the post-reaction mixture is passed through a graphite column and finally the radioactivity of the flow-through is measured. This strategy allows us to specifically assign the detected radioactivity to fucose present in N-glycans.

Our results showed a decrease in the incorporation of fucose derived from the GDP-fucose synthesized *via* the salvage pathway into N-glycans in the SLC35C1 knockout cells, but still the extent of fucose incorporation was more than 23% of the wild-type (Fig. 8A). Surprisingly, incorporation of fucose derived from the GDP-fucose synthesized via the *de novo* pathway (i.e. from mannose) turned out to be nearly completely abolished (6% of the wild-type) (Fig. 8B).

qPCR analysis of expression levels of selected glycosylation-related genes

There is a possibility that some fucosylation-related genes become up- or down-regulated by the exogenously added fucose. Therefore, to complement our metabolic studies, expression levels of selected glycosylation-related genes were analyzed in the control and fucose-fed SLC35C1-deficient cell lines. For the analysis of a larger subset of genes, a ULP probe-based assay was designed (Fig S4). Here, 91 different genes, including NSTs, glycosyltransferases and biosynthetic enzymes involved in metabolism of different monosaccharides (galactose, *N*-acetylglucosamine, mannose, xylose and fucose) were investigated. No statistically significant differences could be assigned for any of the tested genes.

To analyze differences in gene expression between the wild-type and SLC35C1 knockouts in HEK293T and HepG2 cells a SYBR Green-based qPCR assay was performed for six selected genes, i.e. *FCL*, *GMDS*, *FUK*, *FPGT1*, *FPGT2* and *SLC35C2* (Sup tab.1, 2). Similarly to the previous findings, no statistically significant differences between the wild-type and SLC35C1 knockout HEK293T and HepG2 cells (both control and supplemented with exogenous fucose) were observed.

Discussion

In this study we have confirmed the existence of SLC35C1-independent GDP-fucose transport routes in the Golgi complex and determined the intracellular fate of the exogenously supplied fucose. Moreover, we have shown that the SLC35C1-dependent route mainly transports GDP-fucose provided by the *de novo* biosynthetic pathway, whereas the SLC35C1-independent route nearly exclusively translocates GDP-fucose derived from the salvage pathway.

The SLC35C1-deficient mammalian model was for the first time developed and characterized by Hellbusch and coworkers in 2007 [27]. In that study, treatment of cells from different mouse organs with exogenously supplied fucose partially restored glycoprotein fucosylation, which encouraged the authors to propose the existence of an alternative, SLC35C1-independent GDP-fucose transport mechanism. However, the improvement in fucosylation was demonstrated using only a single method, i.e. lectin-based flow cytometry, and no intermediate metabolic steps, e.g. conversion of fucose into GDP-fucose, have been investigated.

The study presented here in multiple aspects extends the previously conducted research. First of all, the improvement in fucosylation caused by supplementation of the culture medium with millimolar concentrations of fucose was precisely determined to be ~77% by our self-developed quantitative HPLC-based approach. Moreover, we showed that also nanomolar concentrations of exogenous fucose are sufficient to observe its incorporation into N-glycans in the knockout cells. Furthermore, we determined the extent to which exogenous fucose is transported into the cytoplasm and how it contributes to the increase of the concentration of the intracellular GDP-fucose (the extracellular fucose, intracellular fucose and intracellular GDP-fucose were shown to exist in a 5 mM / 1 mM / 0.2 mM equilibrium). Finally, we showed that the SLC35C1-independent Golgi GDP-fucose transport systems preferentially use the nucleotide sugar pool derived from the salvage pathway, which we consider the main outcome of this study.

In this study we have developed a quantitative HPLC-based approach allowing for the very precise determination of the level of core fucosylation of N-glycans. This form of fucosylation, mediated by a single Fut8 enzyme, is present in many cell types including HEK293T and HepG2 which were selected as our model. Moreover, it is easy to study due to the well-established procedures of N-glycan isolation and HPLC analysis. As shown by our data, the level of core-fucosylated N-glycans in the wild-type HEK293T and

HepG2 cell lines is high (~80%) but does not reach 100%, giving a possibility to potentially observe a further increase in fucosylation, i.e. over-fucosylation, upon fucose treatment. On the other hand, in these cell lines the level of core-fucosylated structures is high enough to make a clear distinction between the wild-type and the SLC35C1 knockout phenotypes. To conclude, the choice of cell lines was dictated by the high percentage of core-fucosylated N-glycans they produce, which in turn was demanded by the quantitative HPLC-based approached we employed.

Using our quantitative HPLC-based approach we showed that the core N-glycan fucosylation is significantly compromised in the SLC35C1-deficient cells. However, some residual fucosylation could still be detected in these cell lines. The SLC35C2 protein is also specific for GDP-fucose. Thus, its activity could potentially compensate for the lack of SLC35C1 in the single knockout cells. Here we showed that this is not the case as knocking out the *SLC35C2* gene in the SLC35C1-deficient cells did not make the fucosylation defect any more severe. There results suggest that there must be yet another system responsible for the SLC35C1-independent GDP-fucose import into the Golgi lumen.

Strikingly, supplementation of the culture medium with millimolar concentrations of fucose caused a substantial improvement of core N-glycan fucosylation in both single SLC35C1 and double SLC35C1/SLC35C2 knockout cells. In contrast, in the wild-type cells fucose treatment did not cause any further improvement in fucosylation, which is in line with the results obtained by Moriwaki et al. [33] who did not observe any increase in AAL reactivity with glycoproteins produced by the wild-type Hep3B cells supplemented with up to 5 mM fucose. This finding additionally supports our assumption that SLC35C1 mainly utilizes GDP-fucose produced by the *de novo* pathway, whereas GDP-fucose synthesized *via* the salvage pathway does not appear to be an optimal source of this nucleotide sugar in the wild-type cells, even if the latter is present in a large excess. We also hypothesize that the residual fucosylation detectable in the knockout cells is derived from GDP-fucose produced by the salvage pathway, which is not the main source of this nucleotide sugar in the wild-type cells. We believe that if the SLC35C1-independent GDP-fucose transport system used the nucleotide sugar substrate produced by the main biosynthetic pathway (i.e. *de novo*), the level of core fucosylated N-glycans in the knockout cells would be much higher.

It should be emphasized that fucose treatment of the LADII patients and SLC35C1-deficient cells can only be successful if the following requirements are fulfilled: (i) fucose must efficiently enter the cells, (ii) after entering the cell fucose must be readily converted into GDP-fucose *via* the salvage pathway and (iii) GDP-fucose must reach the Golgi lumen to become available for the catalytic centers of fucosyltransferases. Importantly, quantifitation of intracellular GDP-fucose concentration in fucose-fed SLC35C1 knockout cells was not attempted in the previous studies. To the best of our knowledge, the changes in the GDP-fucose content in response to exogenously supplied fucose was examined only by Moriwaki et al. in the wild-type Hep3B cells [32] and, more recently, by Sosicka et al. in the wild-type HepG2, CHO and Huh7 cells [33]. In the first study, the range of analyzed fucose concentrations was between 0 and 5000 μM. However, these results cannot be compared with the ones obtained in this study as both procedures differed in several aspects including the cell line used and the method for nucleotide sugar detection (Moriwaki et al. [33] used an indirect, enzyme-based detection and did not attempt to determine intracellular GDP-fucose concentration, whereas we performed a direct detection followed by estimation of intracellular GDP-fucose concentration). On the other hand, Sosicka et al. tested only one concentration of exogenous fucose (50 μM) [33]. Importantly, neither of these studies attempted to determine the intracellular GDP-fucose concentration in fucose-fed SLC35C1 knockout cells, which is crucial for our understanding of the responsiveness of these cells to exogenous fucose.

Here, we determined GDP-fucose concentrations in the control and fucose-fed wild-type and knockout cells. We found that the baseline concentrations of GDP-fucose were similar in the wild-type and knockout cells, whereas a remarkable increase could be observed upon fucose treatment in all the cell lines analyzed. In native conditions, the salvage pathway was shown to play only negligible role in the overall GDP-fucose production. Here we show that the capacity of this pathway is very high, i.e., the corresponding enzymes are able to process significantly greater amounts of the primary substrate than are normally present in the cell. However, our data exclude the possibility that the exogenously added fucose triggers a strong up-regulation of expression of the enzymes acting in this pathway as we did not observe any significant changes in the relative levels of the corresponding transcripts between the control and fucose-fed SLC35C1 knockout cells.

Our results clearly show that the therapeutic approaches for CDGs associated with impaired NST activity should aim for a drastic increase in the intracellular concentration of the corresponding nucleotide sugar substrates. It should be noted that treatment of these CDGs by oral monosaccharide supplementation can only be successful if the *Km* of an enzyme initiating the corresponding

salvage pathway is sufficiently high. Otherwise, the treatment would simply be ineffective. Fucokinase is the first enzyme acting in the salvage pathway of the GDP-fucose biosynthesis. Importantly, in the case of fucokinase purified from pig kidney *Km* for fucose was determined to be as high as 27 μM [32]. This explains why sub-millimolar and millimolar concentrations of exogenous fucose are required to efficiently stimulate GDP-fucose synthesis and rescue N-glycan fucosylation in SLC35C1-deficient cells.

Given the fact that fucose treatment nearly completely rescued the fucosylation defect in the SLC35C1-deficient cells, it appears surprising that fucose-based therapy turned out to be ineffective for some of the LADII patients. There are two possible explanations for this phenomenon. First, the non-responsive LADII patients might bear additional mutations outside the *SLC35C1* gene that affect the performance of the fucosylation machinery. The other possible explanation is that the presence of certain mutant *SLC35C1* variants is somehow more deleterious to the cells than the absence of the protein.

Regardless of the improvement of fucosylation in the SLC35C1-deficient cells treated with millimolar concentrations of fucose, we have also demonstrated that these cells are able to incorporate fucose supplemented in nanomolar concentrations. This proves that in the knockout cells the salvage pathway is able to fuel the SLC35C1-independent GDP-fucose transport system even at extremely low fucose concentrations.

Since increasing the intracellular concentration of GDP-fucose *via* fucose treatment improved core fucosylation of N-glycans, we wondered if it would be possible to boost the production of this nucleotide sugar by feeding the cells with millimolar concentrations of mannose given the fact that the *de novo* pathway of GDP-fucose synthesis utilizes GDP-mannose as a substrate. However, regardless of the cell line analyzed, mannose treatment did not cause any significant changes in the GDP-fucose concentration. This can be partially explained by the fact that mannose is converted to a variety of different metabolites. Although in mannose-fed cells a statistically significant increase in the GDP-mannose concentration was demonstrated, this did not translate into a similar increase in the GDP-fucose level. We therefore hypothesize that both in the wild-type and knockout cells the *de novo* pathway operates with a nearly maximum efficiency and it is impossible to improve its performance by increasing the amount of its primary substrate, i.e., GDP-mannose. Based on these findings it can be concluded that treatment of LADII patients with mannose wouldn't be an attractive alternative to fucose feeding.

Based on our results we propose the existence of three different GDP-fucose transport systems in the Golgi membrane. The first one is SLC35C1-dependent and mainly utilizes the nucleotide sugar pool derived from the *de novo* pathway. The other two are not dependent on SLC35C1 and mainly use the nucleotide sugar pool synthesized in the salvage pathway. However, the first of them works even under very low (nanomolar) concentrations of exogenous fucose that do not cause any increase in the GDP-fucose concentrations, whereas the other requires much higher concentrations of this nucleotide sugar that can only be obtained by feeding the cells with sub-millimolar and millimolar concentrations of fucose. The existence of the latter SLC35C1-independent transport system is strongly supported by the non-linear dependence of the GDP-fucose content on the concentration of exogenous fucose. We hypothesize that this route may not be physiological and is not exclusively specific for GDP-fucose.

The hypothesis raised above assumes the existence of distinct, independent, separate cytosolic pools of GDP-fucose. Such a phenomenon was recently proposed by Sosicka et al. [33] who elegantly demonstrated that different fucosyltransferases utilize distinct GDP-fucose pools derived from distinct fucose sources. We believe that this effect could be executed by a selective cooperation of the different GDP-fucose transport systems with distinct fucosyltransferases (similar to e.g. SLC35C2, which was shown to specifically support O-fucosylation [11, 12]). But the question arises how different Golgi transport systems could discriminate between the GDP-fucose pools derived from distinct metabolic pathways? This might require a physical proximity (or even association) between the enzymes acting in the individual pathways and the corresponding transport systems. Although the predominant Golgi localization of nucleotide sugar transporters is well established, little is known about the precise subcellular distribution of nucleotide sugar synthases. The study performed by Coates et al. postulated cytoplasmic localization of the GDP-mannose and UDP-glucose pyrophosphorylases [35]. This appears to hold true for all the other nucleotide sugar synthases except for the CMP-sialic acid synthetase (CMAS) whose nuclear localization was shown in the same study. However, it is widely believed that cytoplasmic enzymes catalyzing consecutive reactions in the individual pathways are not randomly distributed. Instead, they are rather sequestered to specific cytoplasmic subcompartments where they form functional assemblies that support substrate channeling [36]. It cannot be excluded that the enzymes acting in the GDP-fucose biosynthetic pathways also display such a tendency.

Importantly, GDP-fucose was shown to inhibit the *de novo* pathway in humans [37] and bacteria [38]. At the same time, this pathway is thought to be the main source of GDP-fucose in mammalian cells. Therefore, an immediate delivery of the GDP-fucose synthesized by the *de novo* pathway to the site of its ultimate utilization (i.e., the Golgi lumen) would be highly beneficial as it would ensure the efficient course of the GDP-fucose biosynthesis by shifting the equilibrium of the reaction. Such a scenario could be possible if the enzymes acting in the *de novo* pathway and the main GDP-fucose transporter, i.e., SLC35C1, were located nearby. Although the mammalian fucokinase was shown to be nearly completely inhibited by 60 μM GDP-fucose [34], we did not observe such phenomenon, as we were able to increase the intracellular concentration of GDP-fucose up to ~200 μM by fucose treatment. This may suggest that the GDP-fucose formed in the salvage pathway does not accumulate in the site of its synthesis but instead is immediately channeled to subcompartments in which it is subsequently utilized. Interestingly, the interactions between a plant UDP-glucose 4-epimerase and two UDP-galactose transporters were recently reported [39]. Therefore, it is highly likely that also the enzymes acting in the *de novo* pathway of GDP-fucose biosynthesis are near to the SLC35C1 protein in mammalian cells.

In this study we have confirmed the existence of the alternative, SLC35C1-independent GDP-fucose transport systems in the Golgi complex. We also have shown that SLC35C2 activity is dispensable for this transport to occur. We demonstrated that the exogenously supplemented fucose efficiently enters the cells and is readily converted to GDP-fucose *via* the salvage pathway. Strikingly, the SLC35C1-deficient cells were virtually unable to incorporate fucose derived from GDP-fucose produced by the *de novo* pathway. There are several questions that still need to be answered, e.g. what is the molecular identity of the SLC35C1-independent GDP-fucose transport systems and how different Golgi transport systems discriminate between the nucleotide sugar pools derived from different biosynthetic pathways. Nevertheless, we strongly believe that the findings obtained in this study initiate a brand new chapter in our perception of fucosylation.

Materials And Methods

Cell culturing and gene inactivation

HEK293T cells purchased from ATCC (American Type Culture Collection, CRL-3216) and HepG2 cells purchased from the collection of the Department of Cancer Immunology (Hirszfeld Institute of Immunology and Experimental Therapy, Polish Academy of Sciences) were cultured in Dulbecco's Minimum Eagle Medium (DMEM High Glucose, Sigma-Aldrich) supplemented with 10% fetal bovine serum, 100 U/mL penicillin and 100 μg/mL streptomycin. Cells were kept at 37°C under 5% CO_2.

Ready-to-use Santa Cruz Biotechnology CRISPR-Cas9 kit was used to inactivate *SLC35C1* gene in HEK293T and HepG2 cell lines. Cells were transfected with a mixture of human SLC35C1 double nickase plasmids (sc-410008-NIC-2) using the FuGENE HD transfection reagent (Promega) according to manufacturer's protocol. Next, cells were cultured in DMEM complete medium supplemented with 1 μg/mL of puromycin for three weeks to select transfected cells. After that time, clones were isolated and checked for the presence of the *SLC35C1* transcript using one-step reverse transcription PCR (RT-PCR) with the HEK293T and HepG2 wild-type cells as the controls. Analysis of genomic DNA derived from the SLC35C1-deficient cells was also performed. Primers used in the reactions were listed in Table 1. Next step in confirmation of the *SLC35C1* gene knockout was western blotting.

Inactivation of the *SLC35C2* gene in the SLC35C1 knockout HEK293T cells was performed in the same manner. Santa Cruz Biotechnology CRISPR-Cas9 kit with mixture of human SLC35C2 double nickase plasmids (sc-409264-NIC-2) was applied. Confirmation of the *SLC35C2* gene knockout was performed at both RNA and genomic DNA levels with using the HEK293T wild-type cells as a control. Used primers are listed in Table 1.

Table 1
Primers used in this study.

No.	Primer Name	Primer Sequence 5'-3'	Product Length [bp]
Primers used in RT-PCR analysis with total RNA as a template			
1	F_C1KO	CTTCCCCAGCTTGCGCCTG	133
2	R_C1KO	GCGGCCCACATTGTAGAAGGC	133
3	F_C1/C2KO	GCTTCTCTACTACTGCTTCTC	233
4	R_C1/C2KO	TCAAGCGCCGTCGCCAGAGCT	233
Primers used in PCR analysis with genomic DNA as a template			
5	F_C1KO	CTTCCCCAGCTTGCGCCTG	236
6	R_C1KO	TTGTTCTTCACTGCTTCAGTC	236
7	F_C1/C2KO	ATTTCCCCCTCTTCATGACG	165
8	R_C1/C2KO	TTCTCATCCTATGGTTCCCCA	
Primer used in gene amplification and site directed mutagenesis			
9	F_HAC1	AAAAAGTCGACATGGCATACCCATACGACGTACCAGACT ACGCAATGAATAGGGCCCCTCTGAAGCGGT	-
10	R_HAC1	AAAAAGTCGACTCACACCCCCATGGCGCTCTT	-
11	F_C1_420_PAM	ACGTCGGTGTAGCCTTCTACA	-
12	R_C1_420_PAM	ACTTGAGGCAGAGGTTATTG	-

Generation of cell lines expressing HA-tagged recombinant SLC35C1 protein

A cDNA encoding human SLC35C1 protein (NCBI accession number NM_018389.5) was generated from total RNA isolated from HEK293T wild-type cells. Forward primer contained nucleotide sequence of the HA tag. The amplified sequence was cloned into pSelect-zeo-mcs plasmid vector (InvivoGen) using SalI (New England Biolabs) restriction enzyme. Subsequently, HA-*SLC35C1* mRNA was modified within protospacer adjacent motif region recognized by Cas9 protein by introducing a silent mutation using Q5 Site-Directed Mutagenesis Kit (New England Biolabs) according to manufacturer's protocol. This step was necessary to protect the HA-*SLC35C1* mRNA from the activity of the Cas9 protein in the knockout cells. The primers used for mutagenesis were listed in Table 1.

The SLC35C1 knockout HEK293T and HepG2 cells were transfected with the obtained vector using the FuGENE HD transfection reagent (Promega) according to manufacturer's instructions. Cells were then cultured in DMEM complete medium with the addition of zeocin (400 µg/mL for HEK293T and 200 µg/mL for HepG2) until stable clones were isolated. Cells stably expressing the HA-tagged SLC35C1 were identified by immunofluorescent staining with an anti-HA primary antibody followed by a secondary antibody conjugated with an Alexa Fluor dye. Additionally, confirmation of the expression of the desired protein was done by western blotting.

Western blotting

Cell lysates were separated in 10% SDS-PAGE gels and transferred onto nitrocellulose membranes (Amersham). After the transfer membranes were blocked. Then, specific fragments of membranes were incubated with appropriate primary and secondary antibodies (listed in Table 2). Steps of blocking, antibodies incubation, washing and signal detection were performed as described previously [40].

Table 2
Antibodies used in western blotting analyses.

Antibody	Cat #	Origin	Dilution	Manufacturer
anti-SLC35C1	PA564146	rabbit	1:1000	Thermo Fisher Scientific
anti-HA	ab9110	rabbit	1:1000	Abcam
anti-HSP60	sc-376261	mouse	1:50000	Santa Cruz Biotechnology
anti-GAPDH	ab8245	mouse	1:10000	Abcam
anti-mouse HRP	W402B	goat	1:10000	Promega
anti-rabbit HRP	A0545	goat	1:10000	Sigma-Aldrich

Fluorescence staining

Subcellular localization of the endogenous GDP-fucose transporter and HA-tagged recombinant SLC35C1 protein was determined using primary and secondary antibodies listed in Table 3. Cells were immunostained as described previously [41]. In the case of determination of fucosylation level with biotinylated lectin in the wild-type and SLC35C1-deficient cells, procedure was modified. After fixation, cells were permeabilized for 5 min at RT using 0.1% Triton X-100 in TBS. Non-specific binding sites were blocked with 3% BSA in TBS for 1 h at RT. Then, biotinylated *Aleuria aurantia* lectin (AAL; Vector Laboratories cat # B-1395-1, 1:300) diluted in blocking solution containing 1 mM $CaCl_2$ and 1 mM $MnCl_2$ was added for 1 h at 37°C. Cells were washed with TBS. Slides were then incubated with streptavidin-Cy3 (Sigma Aldrich, 1:500) solution for 1 h at 37°C. The rest of the protocol remained unchanged. The resulting samples were analyzed using a Leica SP8 confocal microscope and the obtained images were processed using an ImageJ software.

Table 3
Antibodies used in immunofluorescence staining experiments.

Antibody	Cat #	Origin	Dilution	Manufacturer
anti-GM130	610823	mouse	1:100	BD Biosciences
anti-calnexin	ab75801	rabbit	1:100	Abcam
anti-SLC35C1	PA564146	rabbit	1:100	Thermo Fisher Scientific
anti-HA	ab9110	rabbit	1:100	Abcam
anti-HA	26183	mouse	1:100	Thermo Fisher Scientific
anti-rabbit Alexa Fluor 488	A21206	donkey	1:200	Life Technologies
anti-mouse Alexa Fluor 568	A10037	donkey	1:200	Life Technologies
anti-mouse Alexa Fluor 488	A21202	donkey	1:200	Life Technologies
anti-rabbit Alexa Fluor 568	A10042	donkey	1:200	Life Technologies

N-glycan analysis

Control and fucose-fed (5 mM, 24 h) cells were lysed and treated with acetone to concentrate proteins. Proteins were then dissolved and enzymatically deglycosylated. Released glycans were purified, labeled with 2-AB and analyzed as described previously [40]. Obtained glycans were subjected to MALDI-TOF analysis.

O-glycan analysis

Control and fucose-fed (5 mM, 24 h) cells were cultured in medium with 5% fetal bovine serum with an addition of peracetylated O-glycan precursor ($Ac_3GalNAcBn$) for 3 days. Subsequently, O-glycans contained in the culture medium were purified according to an adopted method described by Kudelka et al [29]. The obtained glycans were subjected to MALDI-TOF analysis.

MALDI-TOF mass spectroscopy analysis of N- and O-glycans

Prior to MALDI-TOF analysis, 2-AB-labeled N-glycans were desialylated using α2-3,6,8,9-neuraminidase A (New England Biolabs) and purified in the manner reported previously [40]. Both N- and O-glycans were analyzed in a positive-ion mode as described previously [42].

Analysis of SEAP-derived N-glycans

Cells were transiently transfected with 6xHis-SEAP construct using the FuGENE HD transfection reagent (Promega) according to manufacturer's recommendations. Medium containing secreted protein was collected. The SEAP reporter glycoprotein was subjected to further purification following the protocol described by Olczak and Szulc [28]. Then, isolated N-glycans were labeled with 2-AB and analyzed as described previously [40].

Preparation of RNA

Total RNA was extracted from ~3.2 x 10^6 cells (HEK293T, HepG2) using the Total RNA Mini Kit (A&A Biotechnology, Gdynia, Poland). Isolated RNA was treated with DNase I (A&A Biotechnology) and purified using the Clean-Up RNA Concentrator Kit (A&A Biotechnology). RNA integrity was verified spectrophotometrically.

SYBR Green-based quantitative RT–PCR

Reverse transcription was carried out on 1 µg of total RNA using a SensiFAST cDNA Synthesis Kit (Bioline). PCR was carried out using the Luna Universal qPCR Master Mix (New England Biolabs) and a LightCycler 96 instrument (Roche). The amplification reaction comprised initial denaturation at 95°C for 1 min and followed by 45 amplification steps (denaturation at 95 ℃ for 15 s; primer annealing and extension at 60 ℃ for 30 s). The melting curves were analyzed to monitor the quality of PCR products. Relative quantification of expression of respective genes was determined by the ΔΔCq method using human glyceraldehyde-3-phosphate dehydrogenase (GAPDH; NM_002046.7) as a reference. Three independent experiments (biological replicates) were performed to test each experimental condition and each sample was run in three technical replicates. Hence, in total 3x3=9 runs were executed per one experimental condition. No template controls were included on each reaction plate to check for contamination. Negative controls consisting of untranscribed RNA (no-RT controls) were performed to check for genomic DNA contamination. All primers used in this study are listed in Table 4.

Table 4
List of primers used in SYBR Green-based quantitative RT-PCR.

Gene	NCBI Accession	Forward Primer	Reverse Primer
FX	NM_003313.3	GACAAGACGACCTACCCGAT	GTTCTGCACGTCGATCATCC
FUK	NM_145059.2	GACTGTGGCAGGGCTTTCA	CAGCCGATAGGTCATGATGG
FPGT1	NM_003838.4	GGGTGACATTGCCGATCTTA	CCAAAGCCTGCAGAAAGTCA
FPGT2	NM_001199328.2	GGAGTCTGTTTCCTGTCATGC	CAAACTGGGAAAATGCGTG
GAPDH	NM_002046.7	AGGTCGGAGTCAACGGATTT	TGACAAGCTTCCCGTTCTCA
GMDS	NM_001253846.1	GCCATGCCAAGGACTATGTG	TCTCGACAAATTCCCGGACA

Universal ProbeLibrary-based quantitative RT-PCR

Preparation of cDNA.

cDNA was produced using Transcriptor First Strand cDNA Synthesis Kit (Hoffmann-La Roche, Basel, Switzerland) according to the manufacturer's instructions. Total RNA (4 µg) extracted from HEK293T cells was mixed with 2 µL of 50 pmol/µL anchored-oligo(dT)18 primer and supplemented with PCR-grade water up to 26 µL final volume. The template-primer mixture was incubated in a thermal block cycler with a heated lid for 10 minutes at 65 ℃ to denature RNA secondary structures and cooled on ice. Subsequently, 5x concentrated Transcriptor Reverse Transcriptase Reaction Buffer (8 µL), 40 U/µL Protector RNase Inhibitor (1 µL)

and Deoxynucleotide Mix (10 mM each; 4 µL) and 20 U/µL Transcriptor Reverse Transcriptase were added. Final reaction mixture (40 µL) was incubated in a thermal block cycler with a heated lid for 30 minutes at 55 ℃ and inactivated for 5 minutes at 85 ℃.

Quantitative PCR procedure

qPCR reaction mixture was assembled at room temperature by mixing cDNA (40 µL) obtained in the previous step with PCR-grade water (960 µL) and 2x concentrated LightCycler 480 Probes Master (Roche; 1 mL) and pipetted into a 96-well RealTime ready Custom Panel plate (Roche; 20 µL per well). The plate was sealed with LightCycler 480 Sealing Foil (Roche) and rotated in a horizontal position for 5 minutes at 1000 rpm to dissolve primers and probes lyophilized on the bottom of the Custom Panel plate wells. The plate was spun down in a centrifuge equipped with a 96-well plate swing-bucket rotor to remove any potential air bubbles and subjected to the qPCR experiment using LightCycler 96 instrument (Roche). The PCR reaction was initiated by a 10-minute pre-incubation at 96 ℃ and followed by 45 amplification steps (95 ℃ for 10 s; 60 ℃ for 30 s; 72 ℃ for 1 s).

Custom Panel qPCR plates

qPCR assays (primer pairs and probes) were purchased from Roche and supplied in a lyophilized form in 96-well plates. The exact configuration of the plate including assay positions on the plate, assay IDs and gene names, sequences of forward and reverse primers and ULP probe numbers is provided in Table 5. Assays were verified by the supplier to fulfill a number of quality criteria including: (i) PCR efficiency 2.0 +/- 0.2 (equals 100 +/- 10%), (ii) Cq of highest cDNA concentration ≤34, (iii) Linear dynamic range of at least 3 logs, (iv) High amplification specificity, no side products in gel analysis, (v) Sigmoidal amplification curve, (vi) Fluorescence intensity of amplification curves between 5 and 50 fluorescence units.

Table 5
Configuration of the qPCR plates.

Position	Assay ID	Gene Name	Forward Primer Sequence	Reverse Primer Sequence	UPL Probe Number
A1	130110	SLC35A1	AACCAGCCCAAGCTACAAAA	GCTATAGCGCCAAACCCTAA	31
A2	124746	SLC35B3	CCCTCACTGGATATTTTGGAAT	TGCTTTTCTTCCTGTTGTCACT	129
A3	136535	SLC35F1	GATGTGCTTGTGGGAAGACA	AGACCAGAAGGTCCCCTACC	32
A4	130973	B4GALT2	CGTCTATGTCATCAACCAGCAT	GCAGTCATAGGCGGCATC	161
A5	148704	GALK2	TCTGCAGGTGTCTGGGAAT	CCCGCTGATAGAGTTTGAAGA	65
A6	148684	B3GNT7	CTTCGTCAACCCCACCAA	ACGAACAGGTTTTCCTGTGG	129
A7	144336	MGAT4A	AACGATTAGAAGATGGCTATTTCAG	GGCTGAAATGGGATTGAGAC	138
A8	119576	POMGNT1	AGTGCTCATCTGCACTGTCAA	GAGCCTTGGCTGTGTCCTT	12
A9	148697	FUT8	TCCCATGGAACCTGGAGATA	CTTTAGAATAGCCATCCCAATGA	5
A10	148719	MAN2A2	ACACCGCAAGGGTTTTGAC	CATCCAGGCCATGGAAAA	117
A11	114041	EXT2	GATCTTCCAGAGAAAGGACCAG	GGATGGAGACCCACCTGAG	69
A12	101144	RPLP0	TCGACAATGGCAGCATCTAC	GCCAATCTGCAGACAGACAC	6
B1	148521	SLC35A2_AG	TGGGATTGATGAACTGTGGA	CGCCCCGATACAGTTAAGG	16
B2	124726	SLC35B4	GCTGCAGTAACGTGATCTTCC	AATGTCACAATGTTCCCACATC	128
B3	136504	SLC35F2	AGGCAAACTCTTCACCTGGA	GCTGTCCCACATATACACAAGG	37
B4	148676	B4GALNT	AAGGGCAATGAGGAAAATCC	GTCCAGGAATTCTGGGTACG	79
B5	116669	GALM	ACTGGCCTGATGCAGTCAAT	GTGTGGTCATACTCCTCACCAG	146
B6	148685	B3GNT8	CTCACTAGTGGCCTGGGAGA	TTTGAGCGTCTGGTTGAATG	95
B7	120178	MGAT4B	ACCTTCCTGACGCTGCTG	ACTCCCGCTGGTAAACGTC	29
B8	148683	UAP1	TCCAATGTGAAATCTCTCCTCTTA	CGATGATTAGAGGTGCATGG	67
B9	148665	POFUT1	GGGTGGCATACTGCTTTGAG	GCCAAAGGGGTTTCCTTC	26
B10	132110	MAN2B1	CTCGCTGGAGCTCATGGT	TCCATTAGTGGCTCCGATACTC	66
B11	148696	EXTL1	GCCCCCTCTGAAGCTCAT	TCATTGCTCCAGAGAACCAA	87
B12	102088	PPIA	TTCATCTGCACTGCCAAGAC	CACTTTGCCAAACACCACAT	158
C1	148562	SLC35A2_ER	GCTCTCTCATGACCCACCTC	TTTGCAAAAACTCAGCTAAGAGATAG	23
C2	148668	SLC35C1	TGCTCACCTGCGGTATCAT	ACGACAGGGTGCCTTCTG	129
C3	132648	SLC35F6	CTCAGCGAAGTGATCACAGG	CGAACTTCTCCTCTAGCACCA	158
C4	148701	B4GALT4	GTGAGGAGCATCCCAAGC	CCCCAAAATATCCACTGTAACG	131
C5	149148	GALT	GCCATGATGGGCTGTTCTA	TGCTGACTCTTATAGGCCTGCT	61
C6	145085	B4GAT1 (B3GNT1)	CCCCTGGGAGCCATTCTA	TCAGGACCTCAAAATCAAACC	51
C7	144311	MGAT4C	GAACGCTATGTTCATACTTTCAAGG	AAGAAAGTCCAATTGTAAGATACCG	92
C8	148680	FPGT	CCCTTGGAGTTCAATATCACG	GTGTTGATCCTCCATTTCCAA	67
C9	139370	TSTA3	GCCTGTTCCGGAATATCAAA	AGGACGTTGTCGTTCATGTG	65

Position	Assay ID	Gene Name	Forward Primer Sequence	Reverse Primer Sequence	UPL Probe Number
C10	148702	GMDS	CCTTTCTATCCCCGGTCAC	ACGGAAGTTCACCACAATCC	43
C11	148672	EXTL2	AGCAAACAGGATGAGAAATCG	GGAAATTGCATTGGTTTCCA	85
C12	102108	ALAS1	GAAATGAATGCCGTGAGGAA	CCTCCATCGGTTTTCACACT	57
D1	134300	SLC35A3	CAGGGATATAACCGACTGACCT	CAGCTATTACAAGGCCTCCAA	124
D2	136533	SLC35C2	TCCTGTATGTCACCGTCTCG	TCCAGCTTGAAGATCAGAGAGA	73
D3	148669	SLC35G2	TGTTTTTGTCCTTGCTGGCTA	TTTCCTGGTAGTCCTGCTTTCT	65
D4	129969	B4GALT5	CCATTCCTCATCACCATCG	CCCTTGCCGTTCTTTTGA	73
D5	148721	A4GNT	GGATGTTGAGGGTATGGTGTAAA	GAAGGATATGTTCAGACACCTGAG	79
D6	116036	GCNT2	TGGAGTGACATGGAAGACAGA	CCGTTTCCATAGATACAAATACCA	75
D7	143919	MGAT5	TGAAAAGAGAAAGCGGAAGAAA	CTTAAATCCAGATTCCTTGGTCA	95
D8	148700	FUK	AGCCGAAGGGAGTTGATTG	GCCGCACTTCCAGTTCTCT	85
D9	122110	MAN1A1	TTGTCATGAATCATATAATCGAACATT	GCTTCAACACCACCATCAAA	93
D10	126626	XYLT1	GACTTCCACCGCTTCCAG	ATTCACCACGGCTTCAAACT	140
D11	148694	EXTL3	GACAGGTGCTGCCTTCTTTC	AGTTCATGGCAATGTCCTCAC	138
D12	102978	control C+	CCTGAGTCCGGATGAACTG	GCCTCCCTCAGTCGTCTCT	148
E1	148670	SLC35A4	GGCCTCCTGGAAGGTTTCT	GCAGACATGAGCAGTCCATTT	44
E2	122731	SLC35D1	GCAAATGGTGCATACGTAAAAC	GTGCATTGTAATAGAGCAGTCCA	33
E3	148674	A4GALT	AAGAAGTACTTTGAGGACATCAACC	CTGGCTCTTCTTGTTCCACA	56
E4	148677	B4GALT7	GAGGACGACGAGTTCTACCG	TGGCGAAATGTCTTGTACCC	24
E5	138883	B3GNT1 (B3GNT2)	CAACGCAGGGAACCAAAC	TTGTCCTCTGGGGGTGTCT	3
E6	115327	GNE	TTGCAGAGGGAGGCAAAA	CTCATCTTTTGGCACTGACATC	31
E7	126319	MGAT5B	CAGTTCATGACCATGTTTCCTC	CCGTCTCGTTGAGCTCCT	165
E8	118442	FUT10	GTGGGCTAATATCAGGCTTCA	GGGCAACTCAGGTGGGTAT	16
E9	144334	MAN1A2	GGACCCGATGAACATAGACAC	CCTTCTCATGATCAGCTCGAA	144
E10	148698	XYLT2	GTACACAGATGACCCGCTTG	ACCGTGTGGAAGAAGGACTC	32
E11	138979	CMAS	TCCCCCTGAAGAACATTAAGC	GGTCTGTCGAAACCCATACAC	81
E12	102127	control C+	GCAAATTCACCAAGAGAGACG	CACGTCGACAGGAACATCAG	1
F1	136492	SLC35A5	ATCTTTGGGAGCGTTCCAG	TCATCACTCTTGGGTTTGGTAA	58
F2	135024	SLC35D2	TTACAATTCAGCCCTGACGA	CCAATGTAGGCAACGGATACA	147
F3	148675	B3GALNT1	CACTGAGATCCCTCAAATGGA	GGCTGAGGTACCACATCACAA	18
F4	138552	C1GALT1	ACTGGAATTACAACTATTATCCTCCTG	AGTGAAAAGAAACTGCAAGATCAG	164
F5	144342	B3GNT3	CTTCTTCAACCTCACGCTCA	ATCATCCCCGTTGAGCAC	51
F6	148681	MGAT1	GAATGACAACGGCAAGGAG	GAAAAAGTCGGTGCGGTAGA	40
F7	148724	NAGK	GGAGCTGCTGAAGGAAGGT	GAGAAGAAGTTCTGAGCCTGGA	37

Position	Assay ID	Gene Name	Forward Primer Sequence	Reverse Primer Sequence	UPL Probe Number
F8	135437	FUT11	TTTGGCAATGTGGAAGAGATT	GGTCCAGACCTTGCCAATAA	5
F9	126260	MAN1B1	CCCGTCTCACAGGGGATAA	TGGATGTGCTGTGTCACCTT	16
F10	148695	CHST1	GGCTCGGAACCCTATGAAG	CCGCGTGTTGTTCTGGAT	105
F11	148729	ENTPD4	ACGACAAGGAGGTTCAGTGG	TGTGACTGGCTCGGAAGG	125
F12	102977	control C+	TCCGTATTCGCATCATGAAC	TCATCCATCTTGTCCACCAC	69
G1	136516	SLC35B1	TGCTGAACATCAACCTTTGG	CTCCCCAGTGAACAGGATTC	3
G2	148731	SLC35D3	CAGCCTCACGCTCTGGTC	AGCGCTTGAAGACCACGTA	111
G3	148679	B3GALT6	AAACCTCACGGCCAAGGT	TTGAGCACGAACTCGAAGG	20
G4	125769	GALE	TGTGCCAGGCAGACAAGA	GGCATGAGGTTGTTGGGTAT	71
G5	144344	B3GNT4	GCGGTAGGAGTGGCCTTT	GAGCAACAGCACAGCCAAG	20
G6	148682	MGAT2	GGAAAGTGCTGGTTCCTCAA	TCTGAGTGGATGGTCTACAGGTT	67
G7	116724	OGT	TCTCAGGCCAGCTCCTATTC	AAAAGCGCACCACTCGTC	5
G8	148664	FUT4	CTATCGCCGCTACTTCCACT	CTCTGTACAGCCTGGCACAC	134
G9	133275	MAN1C1	AGCGGGAGAAAATCAAGGAG	TTTTTCCCCATTGCATAACG	53
G10	148662	CHST5	CGGTTCTCCAGCAAGACAGT	CGGGAGATGATGAAGAGCA	79
G11	148705	ENTPD5	CAGTATGGTGGCAACCAAGAA	GAAGGAACCTCTCTGGACCTC	20
G12	107847	control C-	TGGGTTTTTGTTACCTTTATGGTT	GGAGGTAACATGCAAATAATGTGA	85
H1	148712	SLC35B2	CTGAAGCTGCTCTTCTGTGC	GTCCGTAAAGCGCTCACC	5
H2	136502	SLC35E1	TCCTGGGGGTCTTCCTCTAT	CTTGCTGCTCAGGTCTGCT	72
H3	127546	B4GALT1	GGGAGGAGAAGATGATGACATT	TCTCTTGAGTGGCGGATCAT	114
H4	126912	GALK1	GGAACACACGGACTACAACCA	GACACCAGCCCATCCTTG	21
H5	148673	B3GNT6	GTCCCTGACTGCCAAGACTC	CTGCTGCAGTGCTAAGAAACTC	16
H6	148663	MGAT3	CGCTACAAGCTCTTTCTCATGTT	GGGAAGGTGACATAGGACAGG	12
H7	140486	PGM1	CGAGCAAACTGTCCCTTTGT	CTCACGGATGTGGTCAGAAC	91
H8	117327	FUT7	GGAGACTGTGGATGAATAATGCT	CAGCCACAGGAGCCAGAG	21
H9	129183	MAN2A1	CGAATGGACAGAATCATGGA	GCTTGTCTCAGGGCGAAATA	66
H10	117348	EXT1	CTGCAGCCAAGTCCCAGTA	GCTGGTAGGGGCTTGTCAC	104
H11	148699	SPPL3	CAGGGCTTCTCATCTATGATGTC	CCTTCACCATGACGTTGCTA	111
H12	102422	control C-	TGGGTTTTTGTTACCTTTATGGTT	GGAGGTAACATGCAAATAATGTGA	85

Selection of a reference gene

The entire dataset, i.e. the data from all 8 Custom Panel plates that were run (4 experiments with cDNA from SLC35C1-deficient HEK 293T cells and 4 experiments from SLC35C1-deficient HEK293T cell grown in fucose-supplemented medium) was used to reveal the optimal gene to reference any potential changes in expression level of all other tested genes. The list of candidates included 85 unique assays as out of 96 wells 5 were technical while for 6 genes a criterion of giving a product in all 8 experiments were not met.

The analysis was performed using 4 different algorithms, i.e. GeNorm, NormFinder, BestKeeper and delta-Cq method. The most stable consensus gene was beta-1,4-glucuronyltransferase 1 (B4GAT1).

Quantitative PCR data analysis

To test the null hypothesis that feeding cells with 5 mM fucose does not affect the expression of the tested glycosylation-related genes the SLC35C1-deficient HEK293T cells grown in fucose-supplemented medium (N=4, i.e. 4 biological repetitions or 4 Custom Panel qPCR plates) were compared to the SLC35C1-deficient HEK293T cells supplemented with PBS (also N=4). Relative expression folds were calculated using the ΔΔCq method following Taylor et al. [43]. The results were subjected to the t-test and Benjamini-Hochberg procedure to assess the significance of the gene expression differences in the non-fed and fed cells.

Optimization of fucose supplementation conditions

Three supplementation parameters were optimized, i.e. time of supplementation, frequency of medium exchange and concentration of L-fucose. The first optimizations were carried out in two variants. In the first variant, the wild-type and SLC35C1 knockout cells were cultured in complete medium (DMEM High Glucose, 10% fetal bovine serum, 100 U/mL penicillin, 100 µg/mL streptomycin) with addition of 0.5 mM, 1 mM, 5 mM and 10 mM L-fucose dissolved in phosphate-buffered saline (PBS) for 5 and 12 days and the medium was exchanged every day. In the second variant, the wild-type and SLC35C1 knockout cells were cultured in complete medium with addition of 0.5 mM, 1 mM, 5 mM and 10 mM L-fucose dissolved in PBS for 5 and 12 days but the medium was replaced every other day. As the control, the wild-type and SLC35C1-deficient cells were kept in complete medium supplemented with PBS. Control cells were also cultured in two variants as the fucose-fed cells. After that, cells were collected, lysed and subjected to dot-blotting with AAL to visualize fucosylation level. Procedure of dot blotting is described in the section below.

In the next step, SLC35C1 knockout cells were cultured on glass 8-well microscope slides (Merck) in complete medium with 5 mM L-fucose for 48 h. Cells were fixed after 2, 4, 6, 8, 10, 24, 36 and 48 hour after starting supplementation. Fixed cells were subjected to fluorescent staining with AAL lectin according to the procedure mentioned above.

As the last experiment, the wild-type and SLC35C1 knockout cells were treated with different L-fucose concentrations for different times. Cells were collected and lysed. Cell lysates were subjected to N-glycan extraction performed as described above. Purified and 2-AB-labeled N-glycans were analyzed for α-1,6-fucosylation as described below.

Dot blotting

Whole cell lysates obtained from untreated and fucose-fed cells were applied directly on nitrocellulose membrane (Amersham). Glycans containing fucose were detected using biotinylated AAL (Vector Laboratories cat # B-1395-1, 1:300) as described previously [40]. Lectin attached to glycans was visualized by streptavidin conjugated to HRP (Vector Laboratories, cat # SA-5014-1, 1:50000) by chemiluminescence reaction using Western Lightning Plus-ECL kit (PerkinElmer). Equal protein loading was demonstrated by staining proteins on nitrocellulose membrane with the Ponceau S solution.

Determination of L-fucose concentration in the fucose-fed SLC35C1-deficient cells

Concentration of L-fucose in fucose-fed SLC35C1-deficient HEK293T cells was determined using a commercial kit (L-fucose, Megazyme). Briefly, ~120x10 cells were resuspended in MiliQ water and then sonicated. Next, in order to get rid of proteins from the lysate, ice-cold perchloric acid was added. The mixture was spun down and supernatant was collected. Subsequently, assay sample was prepared by mixing the supernatant with the detection buffer and NADP solution (the latter two were supplied by the kit) in volumes recommended by manufacturer. Mixture was incubated over 3 minutes. After that, L-fucose dehydrogenase suspension (supplied by the kit) was added to the mixture in volume recommended by manufacturer. Finally, the absorbance was measured at 340 nm using a Beckman DU-640 spectrophotometer. Concentration of fucose in the test samples was determined based on a calibration curve prepared for the fucose standard (supplied by the kit).

Radioactive labeling of N-glycans and nucleotide sugars

Cells were cultured in complete medium supplemented with 4 µCi/mL L-[6-^{3}H]-fucose (American Radiolabeled Chemicals, specific activity 60 Ci/mmol) for 24 h or 20 µCi/mL D-[1-^{3}H]-mannose (American Radiolabeled Chemicals, specific activity 20 Ci/mmol) for 48

h to analyze N-glycans. Then cells were harvested and subjected to N-glycan preparation followed by analysis of N-glycan α-1,6 fucosylation. For analysis of nucleotide sugars cells were incubated in complete medium with addition of 4 μCi/mL L-[6-^{3}H]-fucose (American Radiolabeled Chemicals, specific activity 60 Ci/mmol) for 24 h or 167 μCi/mL D-[1-^{3}H]-mannose (American Radiolabeled Chemicals, specific activity 20 Ci/mmol) for 48 h. Cells were collected and nucleotide sugars were extracted as described below.

Analysis of N-glycan α-1,6-fucosylation

Purified, 2-AB-labeled and dried N-glycan pools were dissolved in 25 μL of certified, exoglycosidase free GlycoBuffer 1 (50 mM sodium citrate, pH 6.0; New England Biolabs). Neuraminidase A (40 units per reaction), β-1-4 galactosidase S (16 units per reaction) and β-N-Acetyl-Glucosaminidase S (8 units per reaction) were added, to start digestion. All enzymes were purchased from New England Biolabs. Reactions were performed overnight, at 37°C in air-heated incubator, to avoid evaporation. In these conditions, virtually all complex-type N-glycans were converted to two conserved trimannosyl core structures (fucosylated at the first *N*-acetylglucosamine and non-fucosylated). The post-reaction mixtures were separated on GlycoSep N Plus column (Prozyme) at 40°C. High Resolution gradient #1 (Prozyme manual for the column) was applied, and detection was performed with a fluorescence detector (330 nm excitation, 420 nm emission) connected to a Perkin Elmer Series 200 HPLC gradient system. The percentage of N-glycan core fucosylation was calculated from peak area of fucosylated trimannosyl core compared to area of peak eluted as non-fucosylated trimannosyl structure, using TotalChrom software (Perkin Elmer).

The same procedure of separation was applied for N-glycans released from cells labeled with ^{3}H-fucose. In these experiments, fractions of 8 drops (approximately 230 μL) were collected manually and directly transferred to scintillation vials.

Calculations of the extent of radioactive fucose incorporation were based on radioactivity (expressed in cpm) of radioisotope of known concentration and known specific activity compared to peak areas of standard, 2-AB-labeled, trimannosyl core structures (fucosylated and non-fucosylated) of known concentrations (all standard glycans were purchased from Oxford Glycosystems).

Analysis of N-glycan fucosylation after ^{3}H-mannose and ^{3}H-fucose labeling

Purified, 2-AB-labeled and dried N-glycan pools released from cells labeled with ^{3}H–fucose or ^{3}H-mannose, were resuspended in 25 μL of certified, exoglycosidase free GlycoBuffer 1 (50 mM sodium citrate, pH 6.0, New England Biolabs). Then α1-2,4,6 Fucosidase O (New England Biolabs, 4 Units per reaction) was added to start de-fucosylation. The reaction was performed overnight at 37°C. After digestion, the mixtures were complemented with 250 μL of 1% TFA, mixed and applied to the Graphite Spin Columns (Pierce), previously washed two times with 100 μL of 1 M ammonia, primed by 100 μL of acetonitrile and, finally, equilibrated two times with 100 μL of 1% TFA, each step was finished by centrifugation at 2000 g for 1 minute. Applied samples were bound to the graphite resin in closed spin column for 20 minutes, with periodic vortex mixing. After 20-minute incubation, the columns were centrifuged at 2,000g for 3 minutes and washed 3 times with 100 μL of 5% acetonitrile/water/1% TFA solution. The flow–through and washes (approximalely 550 μL of total volume), containing released, free fucose, were combined and transferred to scintillation vials. Glycans bound to the column were released from spin columns with 3 elutions, each with 150 μL of 60% actetonitrile/water/0.5% TFA. Fractions were combined and transferred to scintilation vials. The last step confirmed the 100% rate of fucosidase digestion with no detectable radioactivity in released N-glycans.

Control reactions for the same procedure were also performed, without fucosidase added to GlycoBuffer 1. This confirmed lack of non-enzyme de-fucosylation during overnight incubations.

HPLC separation of nucleotide sugars

Nucleotide sugars were purified from collected and frozen cells using protocol previously published [30]. Enriched nucleotide sugar pools were separated in ion-pairing, reverse phase HPLC, as described previously [44] with some changes. The column was changed to Interstil ODS-4, 250 x 3 mm, 3 μm particle size, flow rate was established to 0.3 mL/min. Buffer A (100 mM potassium phosphate, pH 6.4 supplemented with 8 mM tetrabutylammonium hydrogen sulphate) was used for equilibration, Buffer B (70% of A plus 30% acetonitrile) was used as an eluent. Separations were performed using the following gradient: 0% for 20 minutes, 0–72% for 25 minutes, 72%-77% for 10 minutes and, finally, equilibrated at 0% of buffer A for 25 minutes. Nucleotide sugar samples were resuspended in MiliQ water.

The sample volumes of 5 µL or less were injected to start separations. The column was connected to Nexera Shimadzu HPLC system. Detection was performed at 254 nm with SPD_M30A Diode Array Detector equipped with HS (high-sensitivity) quartz cell. Calculations of nucleotide sugar concentrations were performed with LabSolutions Software (Shimadzu). Standard, high purity nucleotide sugars were purchased from Sigma-Aldrich. The absolute quantification of nucleotide sugars was performed by comparison of the detected signals to the externally added reference compounds. Next, by referring to the starting number of cells and to the anticipated volume of a single cell (3 and 3.5 pL per cell for HepG2 and HEK293T, respectively), it was possible to estimate the intracellular nucleotide sugar concentrations.

The same procedure of ion-pairing reverse-phase separation was applied for nucleotide sugar pools, previously purified from cells labeled with ^{3}H-fucose and ^{3}H mannose (as described before). In these experiments, fractions of 5 drops (approximately 150 µL) between 26th and 33rd minute of HPLC gradient, were collected manually and directly transferred to scintillation vials. Retention times under separation conditions described above were approximately 27.2 min. and 31.1 min., for GDP-mannose and GDP-fucose, respectively.

Statistical Analysis

Statistical parameters including data plotted (mean ± SD), *P value*s, and statistical tests used are mentioned in Figure Legends. Statistical analyses were performed using Graphpad Prism 6. Data were analyzed by Student's t-test and Benjamini-Hochberg procedure or Welch's correction and by one-way ANOVA with the Tukey post-hoc test.

Declarations

Competing interests

All authors declare no competing interests.

Data availability

The datasets generated during and/or analysed during the current study are available from the corresponding author on reasonable request.

Author contributions

E.S. performed CRISPR-Cas knockouts, cell culture experiments, including ^{3}H labeling and fluorescence imaging, contributed to preparation of the manuscript, B.S. performed CRISPR-Cas knockouts, cell culture experiments, ^{3}H labeling, fluorescence imaging, contributed to preparation of the manuscript, including all figures, D.M.-S. wrote the manuscript and strongly contributed to the literature analysis and data interpretation. M.W. performed qPCR on 96-well plates and took part in manuscript writing and data presentation, W.W. performed RT-qPCR SYBR Green assays and took part in data interpretation, M.O. conceptuated and supervised the research, performed preparation and HPLC separations of N-glycan and metabolite samples, and contribute to preparation of the manuscript. The final version of the manuscript was commented on and approved by all authors

Funding

This work is supported by the National Science Centre (Cracow, Poland), 2016/21/B/NZ5/00144 (to M.O.).

References

[1] A. Varki, R.D. Cummings, J.D. Esko, P. Stanley, G.W. Hart, M. Aebi, A.G. Darvill, T. Kinoshita, N.H. Packer, J.H. Prestegard, R.L. Schnaar, P.H. Seeberger (Eds.), Essentials of Glycobiology, Cold Spring Harbor Laboratory Press 2015-2017, Cold Spring Harbor (NY), ISBN: 9781621821328.

[2] P.D. Yurchenco, P.H. Atkinson, Equilibration of fucosyl glycoprotein pools in HeLa cells, Biochemistry 16(5) (1977) 944-53, doi:10.1021/bi00624a021.

[3] P.D. Yurchenco, P.H. Atkinson, Fucosyl-glycoprotein and precursor polls in HeLa cells, Biochemistry 14(14) (1975) 3107-14, doi:10.1021/bi00685a011.

[4] K. Moriwaki, E. Miyoshi, Fucosylation and gastrointestinal cancer, World journal of hepatology 2(4) (2010) 151-61, doi:10.4254/wjh.v2.i4.151.

[5] T.J. Wiese, J.A. Dunlap, M.A. Yorek, L-fucose is accumulated via a specific transport system in eukaryotic cells, The Journal of biological chemistry 269(36) (1994) 22705-11, doi:10.1016/S0021-9258(17)31703-9.

[6] I. Pastuszak, C. Ketchum, G. Hermanson, E.J. Sjoberg, R. Drake, A.D. Elbein, GDP-L-fucose pyrophosphorylase. Purification, cDNA cloning, and properties of the enzyme, The Journal of biological chemistry 273(46) (1998) 30165-74, doi:10.1074/jbc.273.46.30165.

[7] J.M. Capasso, C.B. Hirschberg, Mechanisms of glycosylation and sulfation in the Golgi apparatus: evidence for nucleotide sugar/nucleoside monophosphate and nucleotide sulfate/nucleoside monophosphate antiports in the Golgi apparatus membrane, Proceedings of the National Academy of Sciences of the United States of America 81(22) (1984) 7051-5, doi:10.1073/pnas.81.22.7051.

[8] N.J. Kuhn, A. White, The role of nucleoside diphosphatase in a uridine nucleotide cycle associated with lactose synthesis in rat mammary-gland Golgi apparatus, The Biochemical journal 168(3) (1977) 423-33, doi:10.1042/bj1680423.

[9] T. Lübke, T. Marquardt, A. Etzioni, E. Hartmann, K. von Figura, C. Körner, Complementation cloning identifies CDG-IIc, a new type of congenital disorders of glycosylation, as a GDP-fucose transporter deficiency, Nature genetics 28(1) (2001) 73-6, doi:10.1038/ng0501-73.

[10] K. Lühn, M.K. Wild, M. Eckhardt, R. Gerardy-Schahn, D. Vestweber, The gene defective in leukocyte adhesion deficiency II encodes a putative GDP-fucose transporter, Nature genetics 28(1) (2001) 69-72, doi:10.1038/ng0501-69.

[11] H.O. Ishikawa, T. Ayukawa, M. Nakayama, S. Higashi, S. Kamiyama, S. Nishihara, K. Aoki, N. Ishida, Y. Sanai, K. Matsuno, Two pathways for importing GDP-fucose into the endoplasmic reticulum lumen function redundantly in the O-fucosylation of Notch in Drosophila, The Journal of biological chemistry 285(6) (2010) 4122-4129, doi:10.1074/jbc.M109.016964.

[12] L. Lu, X. Hou, S. Shi, C. Körner, P. Stanley, Slc35c2 promotes Notch1 fucosylation and is required for optimal Notch signaling in mammalian cells, The Journal of biological chemistry 285(46) (2010) 36245-54, doi:10.1074/jbc.M110.126003.

[13] B. Ma, J.L. Simala-Grant, D.E. Taylor, Fucosylation in prokaryotes and eukaryotes, Glycobiology 16(12) (2006) 158r-184r, doi:10.1093/glycob/cwl040.

[14] Y. Gazit, A. Mory, A. Etzioni, M. Frydman, O. Scheuerman, R. Gershoni-Baruch, B.Z. Garty, Leukocyte adhesion deficiency type II: long-term follow-up and review of the literature, Journal of clinical immunology 30(2) (2010) 308-13, doi:10.1007/s10875-009-9354-0.

[15] A. Etzioni, M. Frydman, S. Pollack, I. Avidor, M.L. Phillips, J.C. Paulson, R. Gershoni-Baruch, Brief report: recurrent severe infections caused by a novel leukocyte adhesion deficiency, The New England journal of medicine 327(25) (1992) 1789-92, doi:10.1056/NEJM199212173272505.

[16] A. Dauber, A. Ercan, J. Lee, P. James, P.P. Jacobs, D.J. Ashline, S.R. Wang, T. Miller, J.N. Hirschhorn, P.A. Nigrovic, R. Sackstein, Congenital disorder of fucosylation type 2c (LADII) presenting with short stature and developmental delay with minimal adhesion defect, Human molecular genetics 23(11) (2014) 2880-7, doi:10.1093/hmg/ddu001.

[17] A. Hüllen, K. Falkenstein, C. Weigel, H. Huidekoper, N. Naumann-Bartsch, J. Spenger, R.G. Feichtinger, J. Schaefers, S. Frenz, D. Kotlarz, T. Momen, R. Khoshnevisan, K.M. Riedhammer, R. Santer, T. Herget, A. Rennings, D.J. Lefeber, J.A. Mayr, C. Thiel, S.B. Wortmann, CONGENITAL DISORDERS OF GLYCOSYLATION WITH DEFECTIVE FUCOSYLATION, Journal of inherited metabolic disease 44(6) (2021) 1441-1452, doi:10.1002/jimd.12426.

[18] Y. Helmus, J. Denecke, S. Yakubenia, P. Robinson, K. Lühn, D.L. Watson, P.J. McGrogan, D. Vestweber, T. Marquardt, M.K. Wild, Leukocyte adhesion deficiency II patients with a dual defect of the GDP-fucose transporter, Blood 107(10) (2006) 3959-66, doi:10.1182/blood-2005-08-3334.

[19] E. van de Vijver, A. Maddalena, Ö. Sanal, S.M. Holland, G. Uzel, M. Madkaikar, M. de Boer, K. van Leeuwen, M.Y. Köker, N. Parvaneh, A. Fischer, S.K. Law, N. Klein, F.I. Tezcan, E. Unal, T. Patiroglu, B.H. Belohradsky, K. Schwartz, R. Somech, T.W. Kuijpers, D. Roos, Hematologically important mutations: leukocyte adhesion deficiency (first update), Blood cells, molecules & diseases 48(1) (2012) 53-61, doi:10.1016/j.bcmd.2011.10.004.

[20] A. Hidalgo, S. Ma, A.J. Peired, L.A. Weiss, C. Cunningham-Rundles, P.S. Frenette, Insights into leukocyte adhesion deficiency type 2 from a novel mutation in the GDP-fucose transporter gene, Blood 101(5) (2003) 1705-12, doi:10.1182/blood-2002-09-2840.

[21] D. Cagdas, M. Yilmaz, N. Kandemir, I. Tezcan, A. Etzioni, Ö. Sanal, A novel mutation in leukocyte adhesion deficiency type II/CDGIIc, Journal of clinical immunology 34(8) (2014) 1009-14, doi:10.1007/s10875-014-0091-7.

[22] N. Cooper, Y.T. Li, A. Möller, N. Schulz-Weidner, U.J. Sachs, F. Wagner, H. Hackstein, S. Wienzek-Lischka, M. Grüneberg, M.K. Wild, G. Bein, T. Marquardt, Incidental diagnosis of leukocyte adhesion deficiency type II following ABO typing, Clinical immunology 221 (2020) 108599, doi:10.1016/j.clim.2020.108599.

[23] K.M. Knapp, R. Luu, M. Baerenfaenger, F. Zijlstra, H. Wessels, D. Jenkins, D.J. Lefeber, K. Neas, L.S. Bicknell, Biallelic variants in SLC35C1 as a cause of isolated short stature with intellectual disability, Journal of human genetics 65(9) (2020) 743-750, doi:10.1038/s10038-020-0764-4.

[24] A. Karsan, C.J. Cornejo, R.K. Winn, B.R. Schwartz, W. Way, N. Lannir, R. Gershoni-Baruch, A. Etzioni, H.D. Ochs, J.M. Harlan, Leukocyte Adhesion Deficiency Type II is a generalized defect of de novo GDP-fucose biosynthesis. Endothelial cell fucosylation is not required for neutrophil rolling on human nonlymphoid endothelium, The Journal of clinical investigation 101(11) (1998) 2438-45, doi: 10.1172/JCI905.

[25] T. Marquardt, K. Lühn, G. Srikrishna, H.H. Freeze, E. Harms, D. Vestweber, Correction of leukocyte adhesion deficiency type II with oral fucose, Blood 94(12) (1999) 3976-85, doi: 10.1182/blood.V94.12.3976.

[26] L. Sturla, R. Rampal, R.S. Haltiwanger, F. Fruscione, A. Etzioni, M. Tonetti, Differential terminal fucosylation of N-linked glycans versus protein O-fucosylation in leukocyte adhesion deficiency type II (CDG IIc), The Journal of biological chemistry 278(29) (2003) 26727-33, doi: 10.1074/jbc.M304068200.

[27] C.C. Hellbusch, M. Sperandio, D. Frommhold, S. Yakubenia, M.K. Wild, D. Popovici, D. Vestweber, H.J. Gröne, K. von Figura, T. Lübke, C. Körner, Golgi GDP-fucose transporter-deficient mice mimic congenital disorder of glycosylation IIc/leukocyte adhesion deficiency II, The Journal of biological chemistry 282(14) (2007) 10762-72, doi:10.1074/jbc.M700314200.

[28]]M. Olczak, B. Szulc, Modified secreted alkaline phosphatase as an improved reporter protein for *N*-glycosylation analysis, PLoS ONE 16(5) (2021) e0251805, doi:10.1371/journal.pone.0251805.

[29] M. R. Kudelka, A. Antonopoulos, Y. Wang, D. M. Duong, X. Song, N. T. Seyfried, A. Dell, S. M. Haslam, R. D. Cummings, T. Ju, Cellular O-Glycome Reporter/Amplification to explore O-glycans of living cells, Nature methods 13(1) (2016) 81–86, doi:10.1038/nmeth.3675.

[30] J. Räbinä, M. Mäki, E. M. Savilahti, N. Järvinen, L. Penttilä, R. Renkonen, Analysis of nucleotide sugars from cell lysates by ion-pair solid-phase extraction and reversed-phase high-performance liquid chromatography, Glycoconjugate journal 18(10) (2001) 799–805, doi:10.1023/a:1021107602535.

[31] W. van Tol, Discovery of the sugar supply pathways for the O-mannosylation of dystroglycan. On the road for treating muscular dystrophy-dystroglycanopathy (doctoral dissertation), Radboud University Nijmegen, the Netherlands (2020), https://repository.ubn.ru.nl/handle/2066/213932.

[32] K. Moriwaki, K. Noda, T. Nakagawa, M. Asahi, H. Yoshihara, N. Taniguchi, N. Hayashi, E. Miyoshi, A high expression of GDP-fucose transporter in hepatocellular carcinoma is a key factor for increases in fucosylation, Glycobiology 17(12) (2007) 1311-1320, doi:10.1093/glycob/cwm094.

[33] P. Sosicka, B.G. Ng, L.E. Pepi, A. Shajahan, M. Wong, D.A. Scott, K. Matsumoto, Z. Xia, C.B. Lebrilla, R.S. Haltiwanger, P. Azadi, H.H. Freeze, Metabolic heritage mapping: heterogenous pools of cytoplasmic nucleotide sugars are selectively utilized by various glycosyltransferases, bioRxiv (2021) 2021.11.03.467160, doi:10.1101/2021.11.03.467160

[34] S. H. Park, I. Pastuszak, R. Drake, A. D. Elbein, Purification to apparent homogeneity and properties of pig kidney L-fucose kinase, The Journal of biological chemistry 273(10) (1998) 5685–5691, doi:10.1074/jbc.273.10.5685.

[35] S. W. Coates, T. Jr Gurney, L. W. Sommers, M. Yeh, C. B. Hirschberg, Subcellular localization of sugar nucleotide synthetases, The Journal of biological chemistry 255(19) (1980) 9225–9229, doi: 10.1016/S0021-9258(19)70550-X.

[36] V. Pareek, Z. Sha, J. He, N. S. Wingreen, S. J. Benkovic, Metabolic channeling: predictions, deductions, and evidence, Molecular cell 81(18) (2021) 3775–3785, doi:10.1016/j.molcel.2021.08.030

[37] F. X. Sullivan, R. Kumar, R. Kriz, M. Stahl, G. Y. Xu, J. Rouse, X. J. Chang, A. Boodhoo, B. Potvin, D. A. Cumming, Molecular cloning of human GDP-mannose 4,6-dehydratase and reconstitution of GDP-fucose biosynthesis in vitro, The Journal of Biological Chemistry 273(14) (1998) 8193-8202, doi:10.1074/jbc.273.14.8193.

[38] R. H. Kornfeld, V. Ginsburg, Control of synthesis of guanosine 5'-diphosphate D-mannose and guanosine 5'-diphosphate L-fucose in bacteria, Biochimica et biophysica acta 117(1) (1966) 79–87, doi:10.1016/0304-4165(66)90154-1.

[39] Y. Zhang, Y. Wang, C. Wang, C. Rautengarten, E. Duan, J. Zhu, X. Zhu, J. Lei, C. Peng, Y. Wang, X. Teng, Y. Tian, X. Liu, J. L. Heazlewood, A. Wu, J. Wan, BRITTLE PLANT1 is required for normal cell wall composition and mechanical strength in rice, Journal of integrative plant biology 63(5) (2021) 865–877, doi:10.1111/jipb.13050.

[40] D. Maszczak-Seneczko, T. Olczak, L. Wunderlich, M. Olczak, Comparative analysis of involvement of UGT1 and UGT2 splice variants of UDP-galactose transporter in glycosylation of macromolecules in MDCK and CHO cell lines, Glycoconjugate journal 28 (2011) 481–492, doi: 10.1007/s10719-011-9348-z.

[41] B. Bazan, M. Wiktor, D. Maszczak-Seneczko, T. Olczak, B. Kaczmarek, M. Olczak, Lysine at position 329 within a C-terminal dilysine motif is crucial for the ER localization of human SLC35B4, PLoS ONE, 13 (2018) e0207521, doi:10.1371/journal.pone.0207521.

[42] B. Szulc, P. Sosicka, D. Maszczak-Seneczko, E. Skurska, A. Shauchuk, T. Olczak, H. H. Freeze, M. Olczak, Biosynthesis of GlcNAc-rich N- and O-glycans in the Golgi apparatus does not require the nucleotide sugar transporter SLC35A3, The Journal of biological chemistry 295 (2020) 16445–16463, doi:10.1074/jbc.RA119.012362.

[43] S.C. Taylor, K. Nadeau, M. Abbasi, C. Lachance, M. Nguyen, J. Fenrich The Ultimate qPCR Experiment: Producing Publication Quality, Reproducible Data the First Time, Trends in biotechnology 37 (2019) 761-774, doi:10.1016/j.tibtech.2018.12.002.

[44] K. Nakajima, S. Kitazume, T. Angata, R. Fujinawa, K. Ohtsubo, E. Miyoshi, N. Taniguchi, Simultaneous determination of nucleotide sugars with ion-pair reversed-phase HPLC, Glycobiology, 20(7) (2010) 865–871, doi:10.1093/glycob/cwq044.

Figures

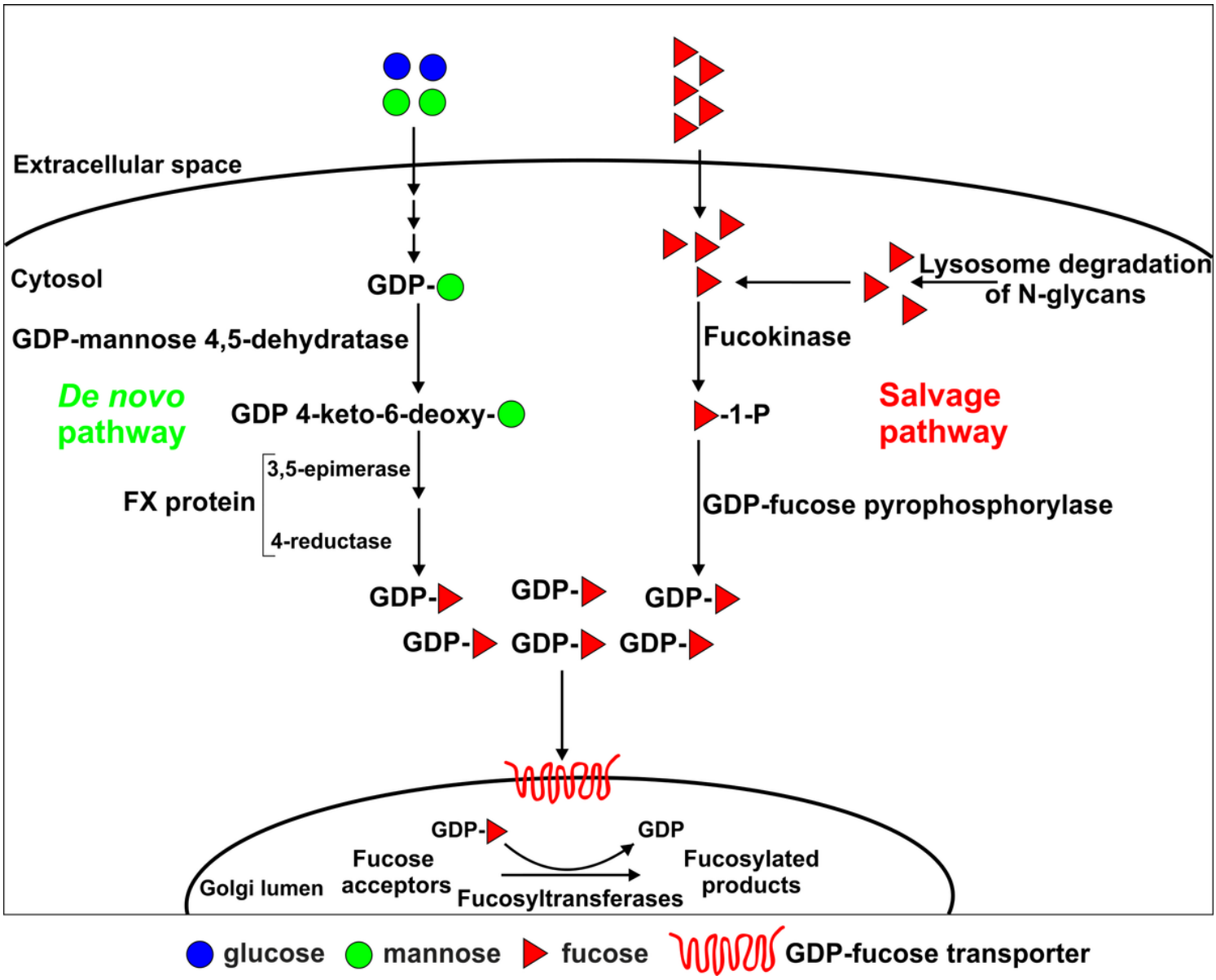

Figure 1

Simplified representation of GDP-fucose metabolism in mammalian cells. GDP-fucose is synthesized in two independent pathways, i.e. de novo (from GDP-mannose) and salvage (from fucose)

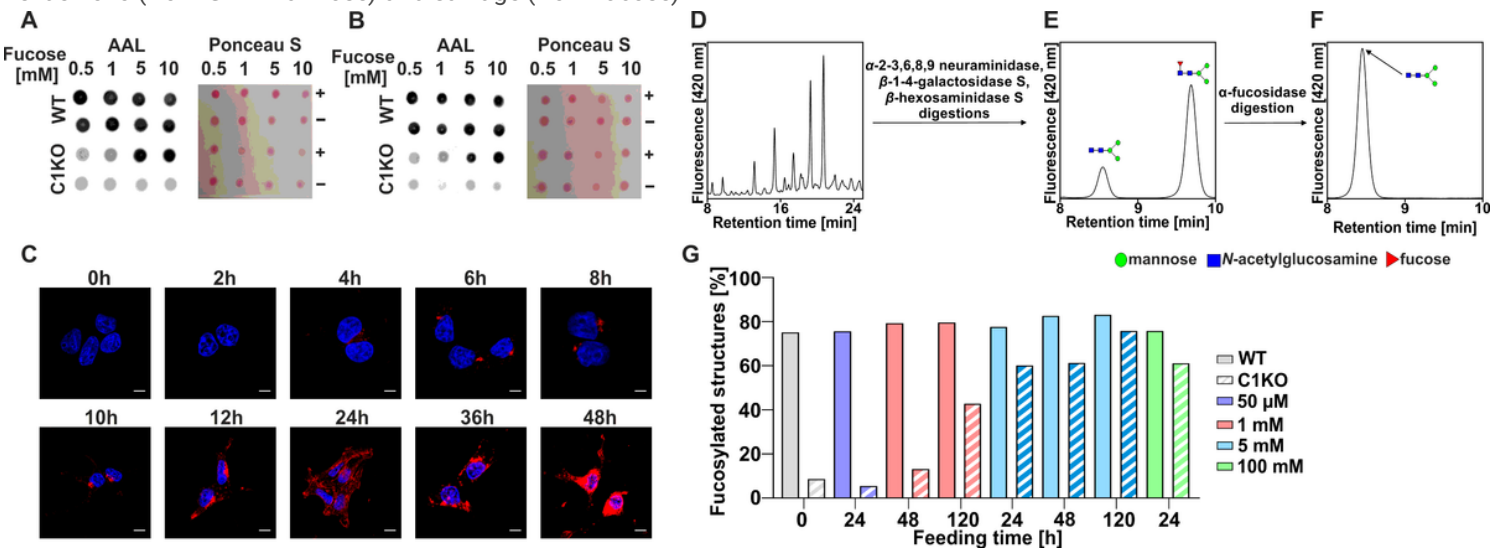

Figure 2

Optimization of the conditions of fucose supplementation. AAL dot blot analysis of the wild-type and SLC35C1 knockout HEK293T (A) and HepG2 (B) cells after 5 days supplementation with (+) or without (-) different fucose concentrations. (C) AAL staining (red) of HEK293T SLC35C1 knockout supplemented with 5 mM fucose during 48 h. Cell nuclei were counterstained with DAPI. Scale bar 10 = µm. (D-F) Schematic representation of our HPLC-based method for quantification of the α1,6 fucosylation of N-glycans. (G) Quantitative analysis of the α-1,6-fucosylation of N-glycans in HEK293T wild-type and SLC35C1 knockout cells supplemented with different fucose concentrations for indicated time periods

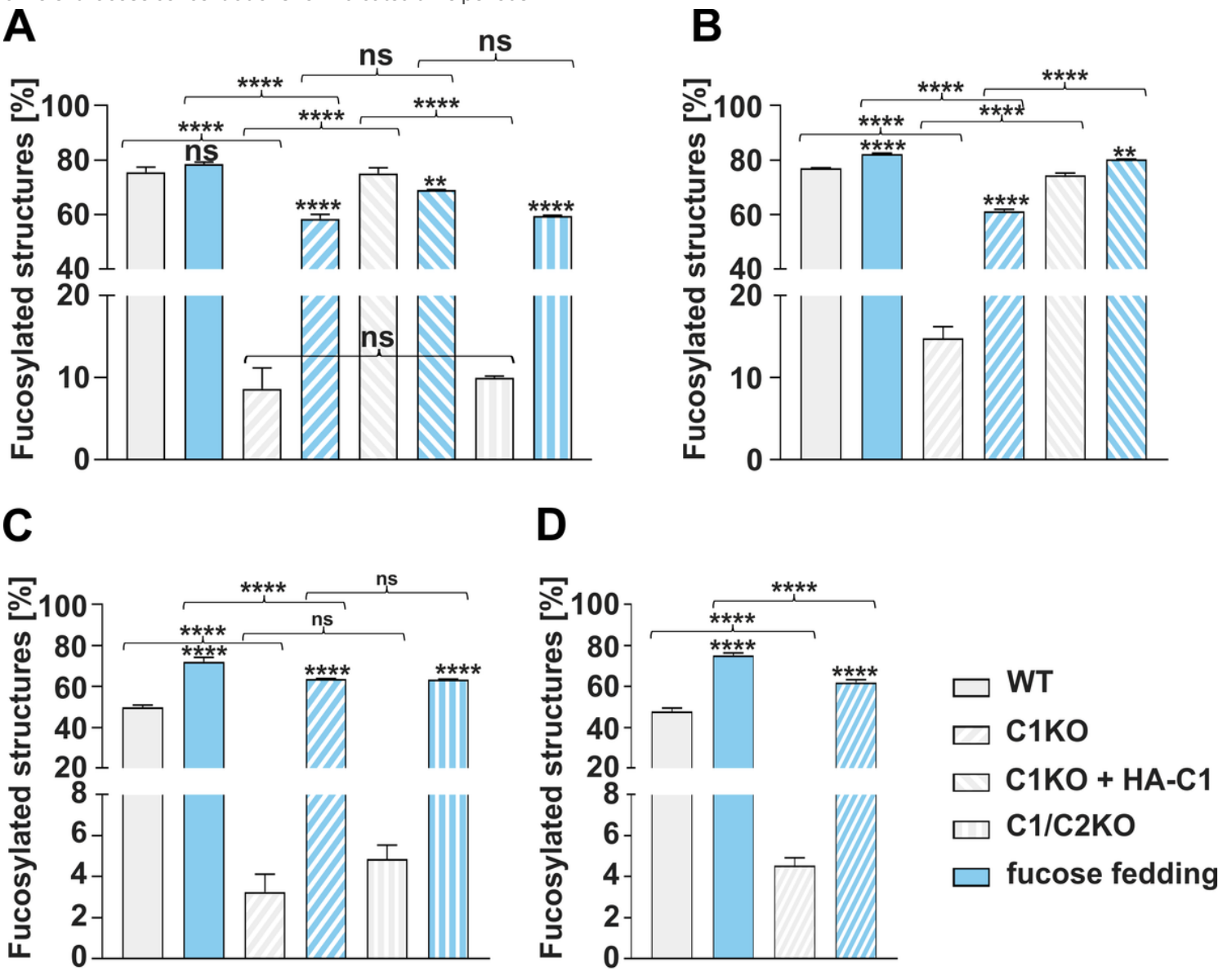

Figure 3

Quantification of the percentage of the core-fucosylated N-glycan structures. HPLC quantification of N-glycans derived from endogenous HEK293T (A) and HepG2 (B) glycoproteins. N-glycans decorating SEAP glycoprotein over-expressed by HEK293T (C) and HepG2 (D) cell lines. ns, not significant; *, $p < 0.05$; **, $p < 0.01$; ***, $p < 0.001$; ****, $p < 0.0001$ as determined using one-way ANOVA with the Tukey post-hoc test. Data are represented as mean ± SEM.

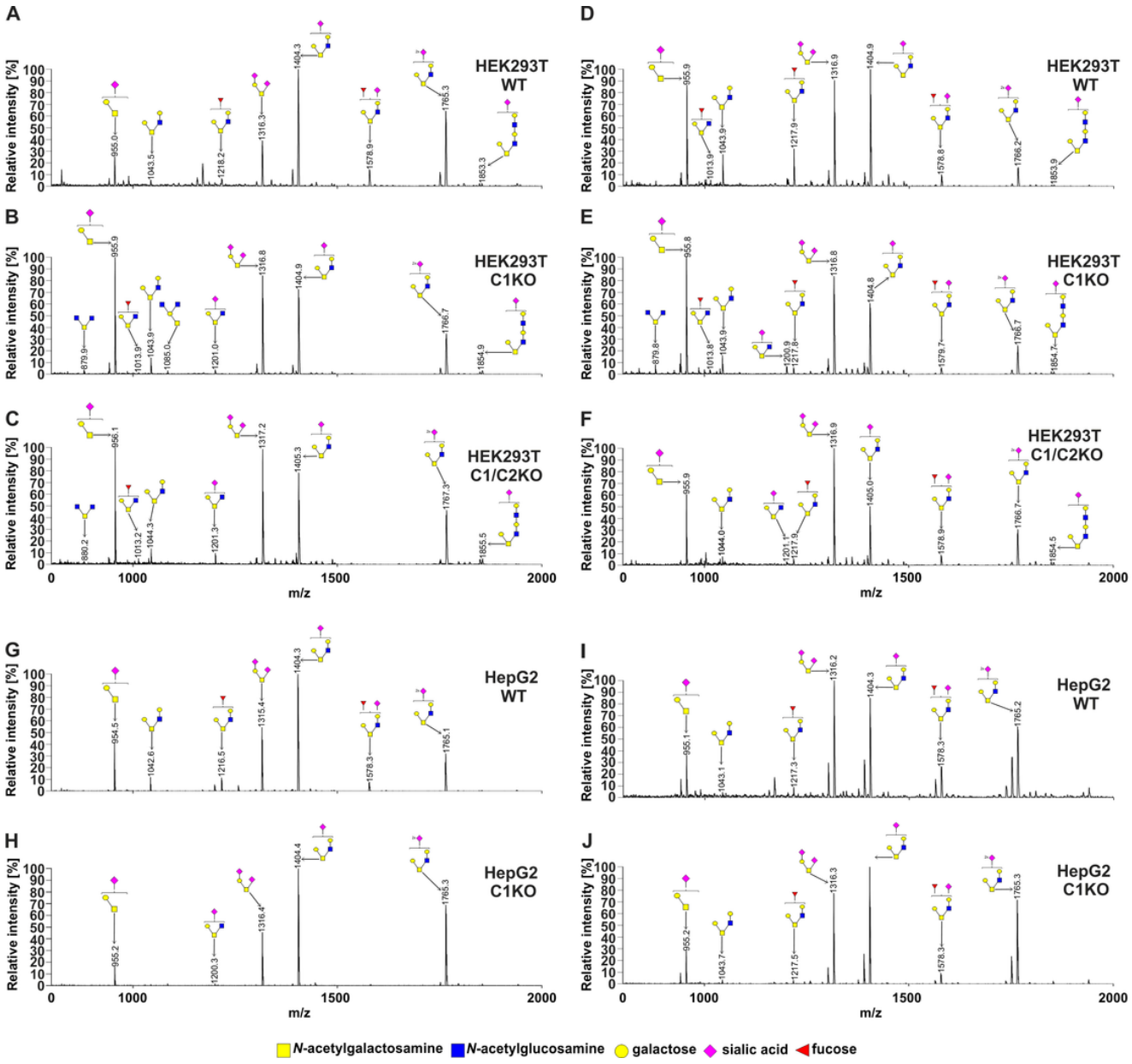

Figure 4

O-glycosylation fingerprinting of HEK293T (A-F) and HepG2 (G-J) cells. MALDI-TOF mass spectra of permethylated mucin-type Bn-O-glycans secreted to the culture medium were permethylated and analyzed in a positive ion mode. Structural assignments based on biosynthetic knowledge were prepared using the GlycoWorkBench tool (2.1; EuroCarbDB).

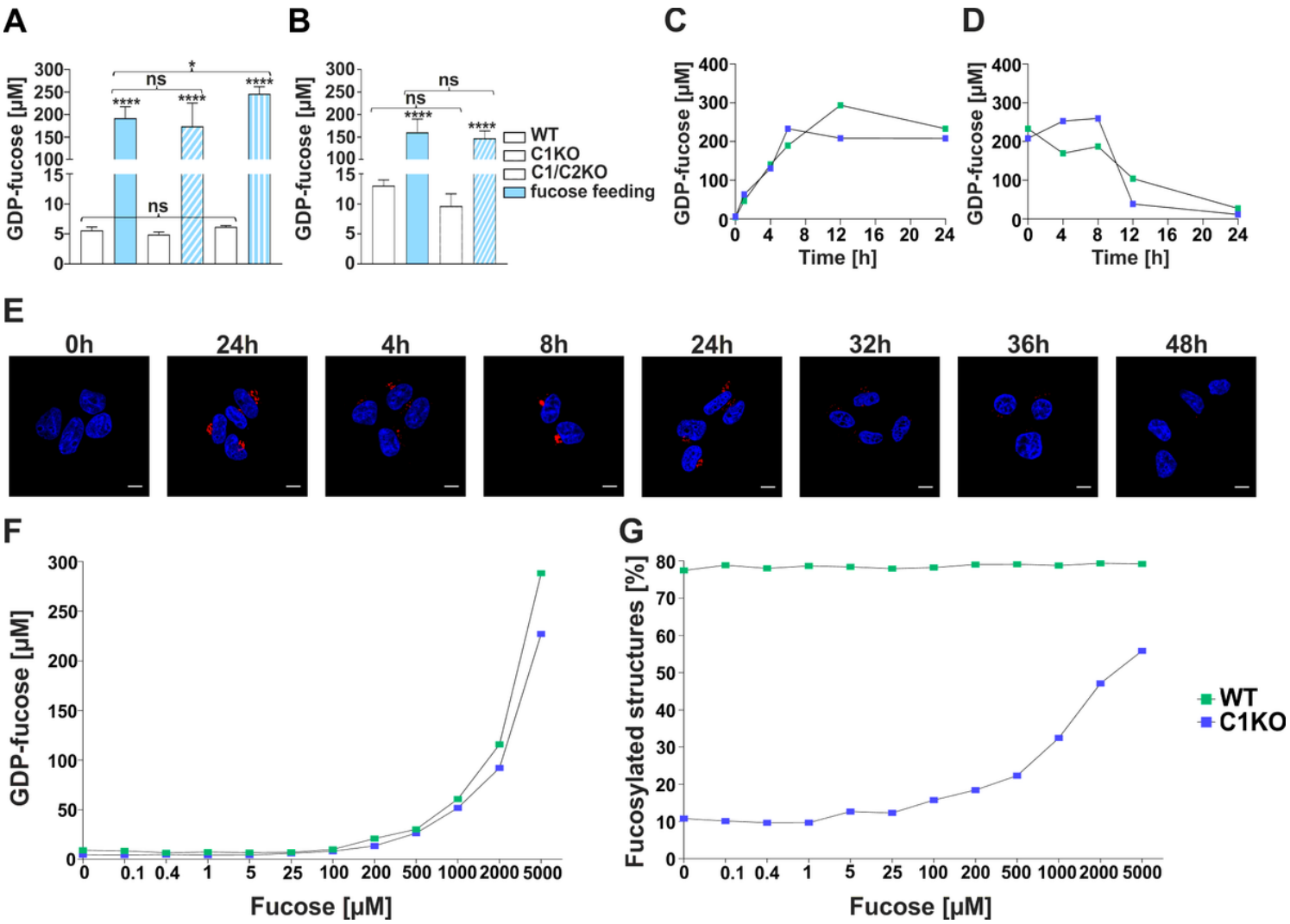

Figure 5

Quantification of the intracellular GDP-fucose concentration. The intracellular GDP-fucose concentration in HEK293T (A) and HepG2 (B) cell lines. ns, not significant; *, p < 0.05; **, p < 0.01; ***, p < 0.001; ****, p < 0.0001 as determined using one-way ANOVA with the Tukey post-hoc test. Data are represented as mean ± SEM (C) Time-course analysis (0-24 h) of the GDP-fucose synthesis in the wild-type and SLC35C1 knockout HEK293T cells fed with 5 mM fucose. (D) Analysis of the GDP-fucose degradation in the wild-type and SLC35C1 knockout HEK293T. The cells were first cultured for 24 h in the presence of 5 mM fucose and then for another 24 h in a fucose-free medium. (E) Disappearance of the fucosylation phenotype visualized by the AAL staining (red). Cell nuclei were counterstained with DAPI. Scale bar = 10 µm. (F) Dependence of the intracellular GDP-fucose concentration on the concentration of the fucose supplemented to the culture medium (HEK293T). (G) Dependence of the percentage of the core fucosylated N-glycans on the concentration of the fucose supplemented to the culture medium (HEK293T)

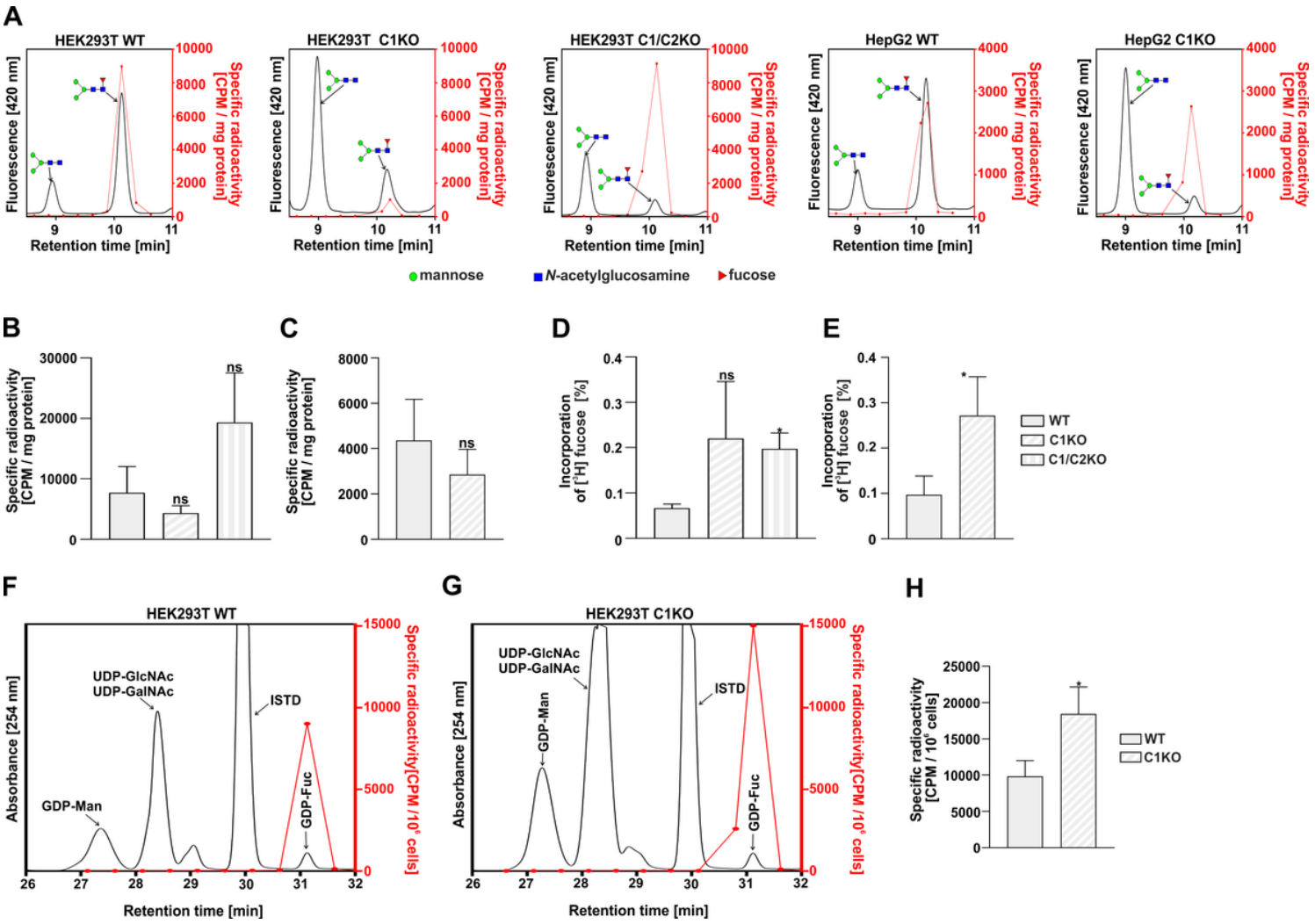

Figure 6

Metabolic labeling of the cellular N-glycans with radioactive fucose. (A) Exemplary representative HPLC chromatograms of the digested N-glycans isolated from the indicated cell lines. The fluorescence signal from the 2-AB-labeled N-glycans (black solid lines) was overlayed with the radioactivity data (red dots and solid lines). The total radioactivity of the fucosylated N-glycans normalized for the amount of the starting material (total protein) from HEK293T (B) and HepG2 (C) cell lines. Percentage of the radioactive fucose incorporated into the fucosylated N-glycans isolated from HEK293T (D) and HepG2 (E) cell lines. To calculate the values the sum radioactivity measured in the HPLC fractions corresponding to the fucosylated species was divided by the total radioactivity of the fucose added to the culture medium. Comparison of the relative incorporation of the radioactive fucose derived from the salvage pathway in the wild-type (F) and SLC35C1 knockout (G) HEK293T cells. (H) The total radioactivity of the GDP-fucose normalized for total number of HEK293T cells. ns, not significant; *, $p < 0.05$ as determined using two-tailed unpaired t-test with Welch's correction. Data are represented as mean ± SEM. ISTD, internal standard (GDP-glucose).

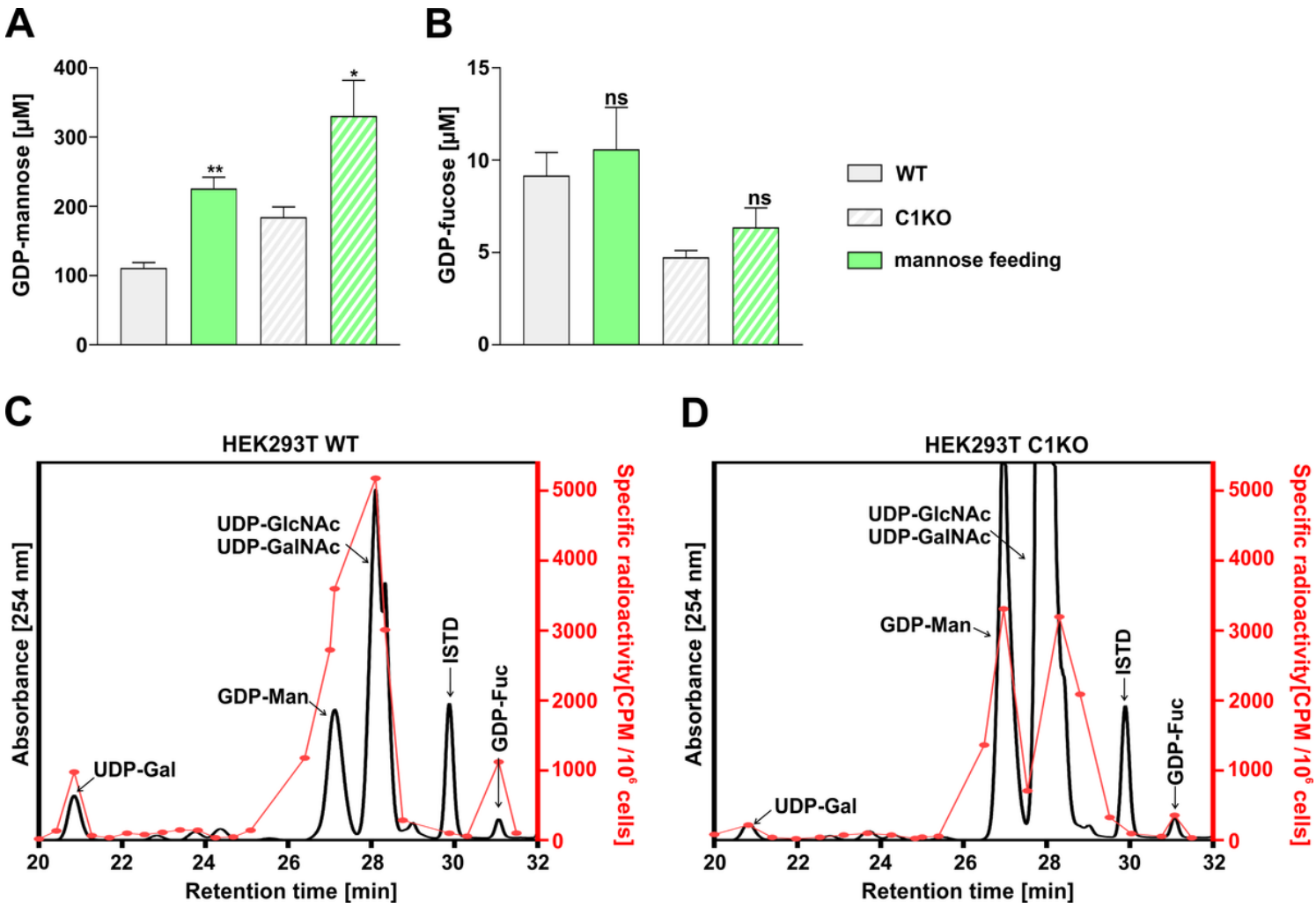

Figure 7

Quantification of the intracellular GDP-mannose and GDP-fucose concentration in cells fed with mannose. Intracellular concentrations of GDP-mannose (A) and GDP-fucose (B) in the wild-type and SLC35C1 knockout HEK293T cells cultured for 48 h in the absence and presence of 5 mM mannose. Comparison of the relative incorporation of the radioactive fucose derived from the de novo pathway in the wild-type (C) and SLC35C1 knockout (D) HEK293T cells. ISTD, internal standard (GDP-glucose). ns, not significant; *, $p < 0.05$; **, $p < 0.01$ as determined using two-tailed unpaired t-test with Welch's correction. Data are represented as mean ± SEM

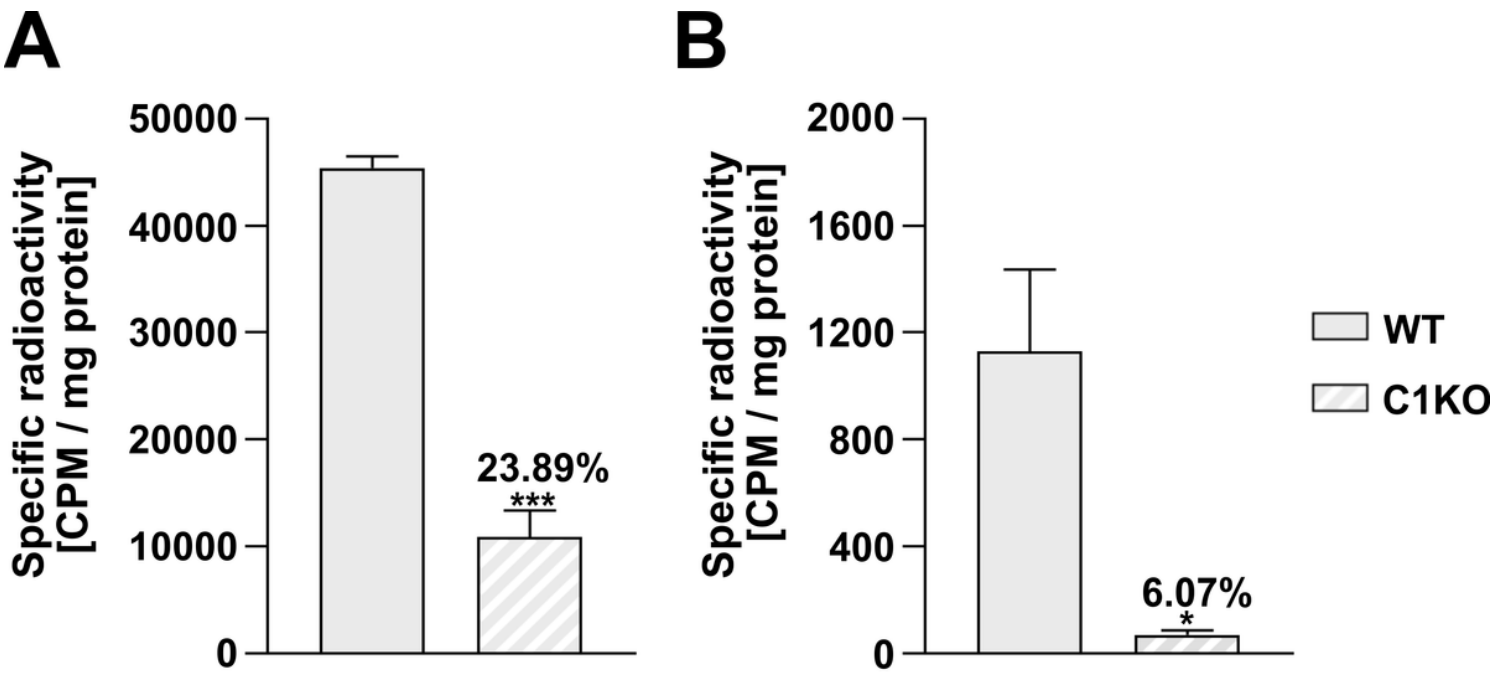

Figure 8

Relative contribution of the de novo and salvage pathways in glycan fucosylation Comparison of the relative incorporation of the radioactive fucose in N-glycans, derived from either the salvage (A) or de novo (B) pathways in the wild-type and SLC35C1 knockout HEK293T cells. The radioactivity was normalized for the amount of the starting material (total protein). ns, not significant; *, $p < 0.05$; ***, $p < 0.001$ as determined using two-tailed unpaired t-test with Welch's correction. Data are represented as mean ± SEM

Supplementary Files

This is a list of supplementary files associated with this preprint. Click to download.

- Supplementarymaterial.pdf